UNIVERSITY OF CALIFORNIA,
IRVINE

The persistent-pursuit and evasion strategies of lionfish and their prey

DISSERTATION

submitted in partial satisfaction of the requirements
for the degree of

DOCTOR OF PHILOSOPHY

in Biological Sciences

by

Ashley Nichole Peterson

Dissertation Committee:
Professor Matthew J. McHenry, Chair
Associate Professor Donovan P. German
Associate Professor Cascade Sorte

2022

DEDICATION

To my Mom, you constantly inspire me with your compassion and creativity, thank you for your unwavering support.

To my Dad, you taught me how to build, fix, and break just about anything, and if I still couldn't do it you taught me how to teach myself.

To Victor, my chef, my research assistant, my teammate and greatest advocate. You keep me motivated and are always dreaming bigger. You can finally call me Doctor.

To friends and family, near and far, your love, encouragement, and laughter kept me sane. I look forward to more adventures.

To Adam and Misty, you took a chance on me. It opened up my world and I will be eternally grateful.

And to my 20 year old self, who in her wildest dreams, never thought she would get this far.

TABLE OF CONTENTS

LIST OF FIGURES

LIST OF TABLES

ACKNOWLEDGMENTS

I am so thankful to have had Dr. Matthew McHenry as my advisor. He allowed me to grow as a scientist, to fail and succeed with grace and patience. I've learned more about coding than I ever imagined, and along the way discovered that I really enjoy the process. Dr. McHenry allowed me to follow my interests while challenging me to expand. His guidance and feedback improved all aspects of my dissertation, and from that I leave with a whole new set of skills.

I thank my doctoral committee members Dr. Cascade Sorte and Dr. Donovan German, and my advancement committee members, Dr. Manny Azizi and Dr. Georg Striedter, for their thoughtful insight and guidance. I am grateful for your support, and your feedback. You pushed me to be a better, well rounded scientist, and exemplify a level of compassion and dedication I aspire to. I also thank Dr. Roi Holzman for hosting me in his lab, and for his guidance and support. He and his lab members made my second chapter a reality. A special thanks the members of the Comparative Physiology Group (past and present) at UCI - you are a large part of why I came to UCI. The training and support of 210 is legendary. I have no doubt that I leave a stronger researcher, writer, and communicator because of your support and feedback.

To the McLabbies, you have made the bad days better and the good days great. I am thankful for all our discussions, recipe swapping, and for the continual moral and intellectual support.

Financial support was provided by the University of California, Irvine, the National Science Foundation Graduate Research Fellowship Program (DGE-1839285) and the European Union's Horizon 2020 research programme, ASSEMBLE Plus project (SR16022018108e1), and from grants awarded to Dr. Mchenry from the National Science Foundation (IOS-1354842 and IOS-2034043) and the Office of Naval Research (N00014-19-1-2035).

VITA

Ashley Nichole Peterson

EDUCATION

Doctor of Philosophy in Biological Sciences **2022**
University of California, Irvine *Irvine, California*

Bachelor of Science in Aquatic and Fishery Sciences **2013**
University of Washington *Seattle, Washington*

Minor of Marine Biology **2013**
University of Washington *Seattle, Washington*

RESEARCH EXPERIENCE

Graduate Research Assistant **2015–2022**
University of California, Irvine *Irvine, California*

Laboratory Technician **2014–2015**
Whitney Lab for Marine Bioscience, University of Florida *St. Augustine, Florida*

Research Technician **2012–2013**
University of Washington and the Department of Natural Resources *Seattle, Washington*

JOURNAL PUBLICATIONS

1. **Peterson, A.N.**, Soto, A.P., McHenry, M.J. 2021. Pursuit and Evasion Strategies in the Predator–Prey Interactions of Fishes. Integrative and Comparative Biology 61: 668–680

2. Akanyeti, O., Thornycroft, P.J.M., Lauder, G.V., Yanagitsuru, Y., **Peterson, A.N.**, and Liao, J.C. 2016. Fish optimize sensing and respiration during undulatory swimming. Nature Communications 7:11044.

3. Bizzarro, J.J., **Peterson, A.N.**, Blaine, J.M., Balaban, J.B., Greene, H.G., and Summers, A.P. 2016. Burrowing behavior, habitat, and functional morphology of the Pacific sand lance (*Ammodytes personatus*). Fishery Bulletin 114:445-460.

CONFERENCE PROCEEDINGS

1. **Peterson, A.N.**, McHenry, M.J. 2021. The persistent predation strategy of the red lionfish (*Pterois volitans*). Virtual Talk. International Coral Reef Symposium

2. **Peterson, A.N.**, McHenry, M.J. 2021. For slow red lionfish, persistence and distance matter when pursuing fast prey. Virtual talk. Integrative and Comparative Biology 61

3. **Peterson, A.N.**, McHenry, M.J. 2019. The coupled strategies of lionfish and prey fish. Integrative and Comparative Biology 59

4. **Peterson, A.N.**, McHenry, M.J. 2017. The kinematics of predation by the red lionfish (*Pterois volitans*). Poster presentation. Integrative and Comparative Biology 57 (suppl 1): e131

5. **Peterson, A.N.** November 19th 2016. Predator-prey interactions of the red lionfish (*Pterois volitans*). Poster presentation. For the 5th Southwestern Organismal Biology (SWOB) SICB Southwest Regional Meeting

6. **Peterson, A.N.**, Akanyeti, O. and Liao, J.C. 2016. Steady swimming kinematics of juvenile Florida Pompano. Poster presentation. Integrative and Comparative Biology 56 (suppl 1): e349

7. Akanyeti, O., Thornycroft, P.J.M., Lauder, G.V., Yanagitsuru, Y., **Peterson, A.N.** and Liao, J.C. 2016. Concerted optimization of propulsion, sensing, and respiration during swimming. Integrative and Comparative Biology 56 (suppl 1): e3

8. Bolla, R., **Peterson, A.N.**, Summers, A.P. and Paig-Tran, E.W.M. 2016. First evidence of cyclonic filtration in Mobulid and Manta ray filter feeders. Integrative and Comparative Biology 56 (suppl 1): e19

9. **Peterson, A.N.**, Akanyeti, O., and Liao, J.C. 2015. The development of a rapid prototyping method for experimental studies of locomotion and flow sensing. Poster presentation, Integrative and Comparative Biology 55 (suppl 1): e314

10. Akanyeti, O., Thornycroft, P.J.M., **Peterson, A.N.**, Lauder, G.V., and Liao, J.C. 2015. Swimming performance of flexible 3-D printed fish. Integrative and Comparative Biology 55 (suppl 1): e3

11. **Peterson, A.N.**, Paig-Tran, E.W.M., and Summers, A.P. 2014. Fluid flow in filter feeding rays: size XL. Poster presentation, Student Competitor, Integrative and Comparative Biology 54 (suppl 1): e330

12. **Peterson, A.N.**, Summers, A.P., and Bizzarro, J.J. 2013. Substrate preference of the Pacific sand lance, *Ammodytes hexapterus*. Poster presentation, Integrative and Comparative Biology 53 (suppl 1): e531

PATENTS

1. Summers, A.P., Paig-Tran, E.W., and **Peterson, A.N.** Cyclonic/cross-flow hierarchical filter, US Patent 20150259219 A1

ABSTRACT OF THE DISSERTATION

The persistent-pursuit and evasion strategies of lionfish and their prey

By

Ashley Nichole Peterson

Doctor of Philosophy in Biological Sciences

University of California, Irvine, 2022

Professor Matthew J. McHenry, Chair

The pursuit of prey is vital to the biology of a predator and many aspects of predatory behavior are well-studied. However, it is unclear how a pursuit can be effective when the prey is faster than a predator. Using kinematic measurements, we considered the strategy of red lionfish (*Pterois volitans*) and devil lionfish (*Pterois miles*) as they pursued a variety of prey fishes. Despite generally swimming slower than their prey, red lionfish and devil lionfish succeeded in capturing prey in 61% and 82% of our experiments. This successful pursuit behavior was defined by uninterrupted motion and a targeting strategy of pure pursuit, characterized by heading towards the prey's position and not the anticipated point of interception. These characteristics comprise a behavior that we call the 'persistent-predation strategy', which may be exhibited by a diversity of predators with relatively slow locomotion. When encountering lionfish, prey avoidance behavior was variable among species, but without a consistency that was predictive of the outcome of an interaction. The coupled nature of these interactions challenge the ability to resolve what aspects of performance matter during predator-prey interactions. To address this challenge, we developed a 2D agent-based mathematical model for a fish predator and an individual prey fish enclosed within a circular arena. We parameterized and tested the predictions of this model with experimental measurements of fish trajectories and performed numerical simulations with a Monte-Carlo approach to predict the trajectories of predator and prey. By manipulating

single parameters, we were able to determine the effect that each parameter had on the outcome of a simulated interaction. We found that metrics related to vigilance and evasion strategy may be more valuable toward evading a slow predator than maximal measure of kinematic performance. This method demonstrates the power of agent-based mathematical modeling for testing hypotheses about the salient features that determine the outcome of predator-prey interactions.

Chapter 1

Red lionfish (*Pterois volitans*) pursue prey with slow persistence

1.1 Abstract

The pursuit of prey is vital to the biology of a predator and many aspects of predatory behavior are well-studied. However, it is unclear how a pursuit can be effective when the prey is faster than a non-cryptic predator. Using kinematic measurements, we considered the strategy of red lionfish (*Pterois volitans*) as they pursued a faster prey fish (*C. viridis*). Despite swimming about half as fast as *C. viridis*, lionfish succeeded in capturing prey in 61% of our experiments. This successful pursuit behavior was defined by three critical characteristics. First, lionfish targeted *C. viridis* with pure pursuit by adjusting their heading towards the prey's position and not the anticipated point of interception. Second, lionfish pursued prey with uninterrupted motion. In contrast, *C. viridis* moved intermittently with variation in speed that included slow swimming. Such periods allowed lionfish to close the distance to a prey and initiate a suction feeding strike at a relatively close distance (< 9 cm).

Finally, lionfish exhibited a high rate of strike success, capturing prey in 74% of all strikes. These characteristics comprise a behavior that we call the 'persistent-predation strategy', which may be exhibited by a diversity of predators with relatively slow locomotion.

1.2 Introduction

A variety of factors affect whether a predator will succeed in capturing its prey. Animals that prey upon evasive organisms must consider the behavior of prey into their hunting strategy. If the predator is relatively slow, then it may employ an ambush strategy to capture prey that unwittingly move within the predator's strike range (e.g., spiders [48], snakes [78, 3, 81], mantis shrimp [27], and fishes [71, 74, 17]). A cryptic predator may alternatively stalk the prey by approaching slowly before striking (e.g., lynx [41], jumping spiders [9], and fishes [44, 70]). If the prey becomes aware of the predator, then a chase may ensue where the outcome is determined by the relative speed and agility of both animals. It is commonly assumed that the predator will have a speed advantage in a pursuit, which allows for an application of missile-targeting models to understand a predator's directional control and effectiveness [31, 14, 50, 52, 68, 37]. However, not all predators are faster than their prey. A prominent example is offered by the Pacific red lionfish (*Pterois volitans*), which is a devastatingly invasive predator to coral reef habitats in the Atlantic Ocean [24]. This fish swims slowly, with its disproportionately large pectoral fins splayed forward. Lionfish exploit their disruptive coloration [77] to ambush small prey within complex habitats, but also actively forage in the water column, where they are likely visible to prey fish [26, 10]. Existing theory does not offer an explanation for the success of a predator that pursues faster prey without the crypsis necessary for a stalking or ambush strategy. In an effort to understand the predation strategy of lionfish, we performed a kinematic analysis of these animals as they preyed upon faster fish (*Chromis viridis*, figure 1.1*a*).

A major component of predatory behavior is the targeting control toward the prey. The bearing angle (figure 1.1*b*) offers a means for distinguishing between the major types of targeting. Predators that direct their swimming towards the prey's position maintain a near-zero bearing angle, which is known as 'pure pursuit' (figure 1.1*b,c*). Pure pursuit requires only that the predator sense the prey's position and is exhibited by animals as

disparate as beetles [40] and fishes [60, 83]. This targeting contrasts predators that attempt to move toward the anticipated point of interception with the prey, which is achieved by targeting known as 'parallel navigation' (figure 1.1*b,d*). Parallel navigation is only possible when the prey is either slower or directed toward the predator (see equation 1.1). In this form of targeting, the predator's bearing is adjusted according to the position and relative velocity of the prey, and therefore requires a higher level of sensory-motor control than what is necessary for pure pursuit. Parallel navigation has been observed in aerial predators like hawks, bats, robber flies, and dragonflies [31, 14, 50, 52, 68, 37], but it is unclear whether fishes are capable of this neuromechanical control [60, 55].

A prey's avoidance behavior necessitates balancing vigilance to a threat against the need to forage, seek mates, defend territories, and other essential behaviors. Reef fishes may therefore tolerate the presence of fish predators, particularly when they can remain in close proximity to a refuge [5, 45, 75, 43]. Predators hovering over a reef may consequently seek opportunities to capture prey, perhaps capitalizing on moments when their vigilance is compromised [33, 86]. Such behaviors have been described in trumpetfish (*Aulostomus maculatus*), cornetfish (*Fistularia commersonii*), and lizardfish (*Synodus variegatus*), when foraging for small reef fishes [44, 70, 6, 86, 7]. When avoidance behavior fails, then a prey's survival may require an evasive maneuver. This may consist of a sharp turn, such as exhibited by birds and other animals in flight [46], or an escape behavior that attempts to dodge a predator's strike [82]. A predator's accuracy and the distance at which a strike is initiated can be decisive factors in the outcome of these interactions [84, 49].

The present study considered multiple aspects of the predatory strategy of lionfish in our kinematic analysis. We compared measurements of bearing against the predictions of pure pursuit and parallel navigation to resolve the species' targeting control. We examined the factors of the prey's behavior that contributed to the lionfish's ability to close the distance

to its target. Finally, we tested how the distance between the animals served as a mediating factor in strike probability and success.

1.3 Material and methods

We recorded the body movement by individual lionfish (*Pterois volitans*, TL = 17.6 cm ±5.0 cm, $n = 5$) as they interacted with individual prey fish (*Chromis viridis*, TL = 3.4 cm ±0.7 cm, $n = 23$, figure 1.1*a*) in a cylindrical tank. We performed a kinematic analysis of these recordings with custom software (in MATLAB v. 2019b, MathWorks, Natick, MA, USA) to test the pursuit strategy of the predators. This software found the center-of-area of each fish body by semi-automated image processing of each video frame near the end (≤ 5 min) of each experiment (figure 1.2*a*). From the trajectories of the two animals, we calculated speed (figure 1.2*b*), distance (figure 1.2*c*), heading, the prey's relative heading (β, equation S1, figure 1.1*b*), and the predator's bearing (ϕ, equation S2, figures 1.1*b*, 1.2*d*–*e*). For each experiment, we found the proportion of time that each fish spent at a near-zero velocity (< 0.01 cm s^{-1}) as a metric of intermittent swimming. Our kinematic measurements were not normally distributed and we therefore analyzed using non-parametric statistics.

We evaluated whether lionfish move with kinematics that are consistent with either pure pursuit or parallel navigation. Pure pursuit was tested by examining whether the 95% confidence intervals (CI) of bearing measurements spanned a zero value [11, 94]. Lionfish bearing angles from individual experiments did not follow a uniform Von Mises distribution (mean kurtosis $k_0 = 2.09 \pm 4.56$, $n = 23$), and were instead skewed toward the circular mean angle (mean skewness $b = 0.003 \pm 0.09$, $n = 23$). To test whether lionfish alternatively moved with parallel navigation, we compared bearing measurements against the bearing predicted

(ϕ_{para}) by the following equation [79]:

$$\phi_{\text{para}} = \sin^{-1}\left(\frac{s_{\text{e}} \sin\beta}{s_{\text{p}}}\right), \tag{1.1}$$

where s_{e} and s_{p} are respectively the speed of the prey and predator. This calculation was only possible for the rare moments when the prey was either slower or directed towards the predator.

We examined how the distance between predator and prey affects the likelihood of a strike and its success. In particular, we compared the distance at which strikes were initiated (d_{strike}), against the closest distance attained between the animals that did not result in a strike, the 'alternative minimum-distance' (d_{alt}). For experiments where a strike occurred, the relationship between d_{strike} and prey capture success was fitted using a binomial logistic regression. See electronic supplemental materials for details on our methodology.

1.4 Results

Lionfish continuously moved towards the prey for the duration of all experiments and successful captured prey in 19 of 23 experiments. A typical experiment concluded when the predator captured an individual after pursuing the prey as it swam around the periphery of the cylindrical tank (figure 1.2*a*). Despite *C. viridis* generally maintaining a greater speed than the predator (figure 1.2*b*), the distance between the animals eventually reduced to a proximity at which the predator initiated a strike (figure 1.2*c*). Throughout the experiments, the lionfish tracked prey with a bearing angle that oscillated around zero, despite the prey's evasive swimming (figure 1.2*d*–*e*). The average bearing for all experiments was indistinguishable from zero (figure 1.3*a*). These results are consistent with a targeting control governed by pure-pursuit. For each experiment, we performed a reduced-major-axis regression that

tested whether the measurements of bearing were similar to the values predicted for parallel navigation. We found that this relationship was significantly different ($p < 0.05$, reduced-major-axis regression) from unity in 21 of 23 experiments (figure 1.3*b*–*d*). Therefore, lionfish generally favored a strategy of pure pursuit by aligning their heading with the line-of-sight.

The pursuit of lionfish was characterized by swimming that was generally slower than the prey. The average lionfish swimming speed (6.36 ± 3.66 cm s^{-1}, $n = 5$, this and all further measurements are reported as Mean ± 1 SD) was roughly half the average speed of *C. viridis* (12.3 ± 10.0 cm s^{-1}, $n = 23$, figure 1.4*a*), but prey generally exhibited greater variation in speed over the course of the experiments (figure 1.4*b*). Both fishes exhibited bouts of slower swimming, but *C. viridis* spent a significantly greater proportion of time swimming at near-zero velocities (< 0.01 cm s^{-1}, figure 1.4*c*).

We examined how the distance between the prey and the predator's rostrum affected the success and likelihood of a strike. Lionfish were highly successful, capturing prey in 74% of experiments in which a strike occurred ($n = 19$), in part because the lionfish initiated their strike within close proximity to the prey. Specifically, 90% of the strikes occurred within 7 cm of the lionfish's rostrum and this preferred strike range corresponded well to the capture success. A binomial logistic-regression fit to our measurements found an even probability of success at a distance of 6.94 cm (figure 1.5*c*). In addition, successful strikes occurred at about 1.3× the distance ($d_{\text{strike}} = 4.84 \pm 1.98$ cm, $n = 14$) of failed strikes ($d_{\text{strike}} = 6.50 \pm 1.38$ cm, $n = 5$, figure 1.5*b*). Up until a strike, the prey succeeded in maintaining their distance from the lionfish. For example, the closest distance attained without a strike ($d_{\text{alt}} = 17.5 \pm 14.5$ cm, $n = 13$, figure 1.5*a*) was about three-fold greater than the mean strike distance ($d_{\text{strike}} = 5.28 \pm 1.83$ cm, $n = 19$).

1.5 Discussion

We found that lionfish employ a predation strategy that succeeds in capturing relatively fast prey without the need for crypsis. This persistent-pursuit strategy capitalizes on a prey fish's periodic pauses in swimming with an uninterrupted slow approach that is targeted directly at the prey's position. This strategy benefits from the deadly effectiveness of the lionfish's suction feeding strike when the prey is in close proximity. Persistent pursuit may help explain the success of lionfish as an invasive predator [24], but this strategy could also apply to a diversity of other relatively slow predators.

A key feature of persistent pursuit is the predator's control of its heading. The lionfish attempted to direct their swimming with the instantaneous position of the prey, which equated to a near-zero bearing angle (figure 1.3*a*). These kinematics are consistent with pure-pursuit targeting, which is also employed by faster fish predators, such as pelagic bluefish (*Pomatomus saltatrix*) and the intermittent-swimming zebrafish (*Danio rerio*) [60, 83]. Deviations of predator bearing away from zero were poorly explained by parallel navigation, suggesting lionfish do not alter targeting behavior to intercept the prey, even in the rare instances when they swim faster (figure 1.3*b*–*c*). Pure pursuit generally follow a longer path length, and hence time to capture, but parallel navigation requires a locomotor system that can overtake evasive prey [38, 40, 60]. The drag-inducing pectoral fins of the lionfish do not lend themselves to such locomotor feats.

The success of a lionfish's strike depends critically on the distance at which it is initiated (figure 1.5*b*–*c*). Suction feeding involves a rapid expansion of the rostrum and low pressure within the buccal cavity to draw in prey that are immediately in front of the mouth [64, 88, 89]. Lionfish chose to strike only when prey were within close range (figure 1.5*a*) and were highly successful (74%, $n = 19$) in capturing *C. viridis*. We identified the distance at which the lionfish showed an even probability of success (6.94 cm) and found that the

probability of capture declined rapidly beyond that range (figure 1.5*c*). These results are perhaps unsurprising, given the spatial limitations of suction feeding [85, 90, 34, 64].

The success of persistent pursuit depends on the prey's behavior. The nearly 2-fold faster swimming of *C. viridis* (figure 1.4*a*) succeeded in maintaining the lionfish at a safe distance until succumbing to the predator's strike (in 19 of 23 experiments). The closest distance between the fish where the lionfish did not strike (d_{alt}) was more than 3-times greater than the mean strike distance (figure 1.5*a*). Therefore, the lionfish generally did not miss an opportunity to strike when *C. viridis* failed to maintain its distance. Although rare, these opportunities were the consequence of frequent instances when *C. viridis* would pause its forward motion (figure 1.4*b*–*c*). The behavioral decisions underlying these decisions cannot be directly quantified, but appear to reflect lapses in vigilance or errors in gauging the predator's proximity. Tropical reef fishes are often reliant on visual cues for predator evasion [59, 53, 69, 29], such as the looming stimulus, increase in the angle subtended on the eye by an approaching object [28, 87]. This stimulus is dependent on the speed of approach and the size of the object, thus a slow approach can be insufficient to trigger an escape response in prey fish [61, 91]. The lionfish's strategy of a slow and persistent approach may habituate prey to their presence and circumvent cues for escape, a potentially useful strategy for vigilant prey [33].

1.6 Summary

We found that lionfish employ a novel behavior for capturing prey that we call the persistent-pursuit strategy. Our experiments revealed how this strategy permits lionfish to succeed as predators, despite swimming slowly and lacking crypsis. Persistent-pursuit includes pure-pursuit targeting with consistent forward motion and an effective predatory strike. *C. viridis* universally attempted to evade the lionfish, but most ultimately failed by pausing their

swimming long enough that the lionfish succeeded in closing the distance. The predatory strike exhibited a high capture success largely due to the close proximity at which is was initiated. Persistent pursuit may be an effective predatory strategy for a diversity of slow and non-cryptic predators.

1.7 Figures and tables

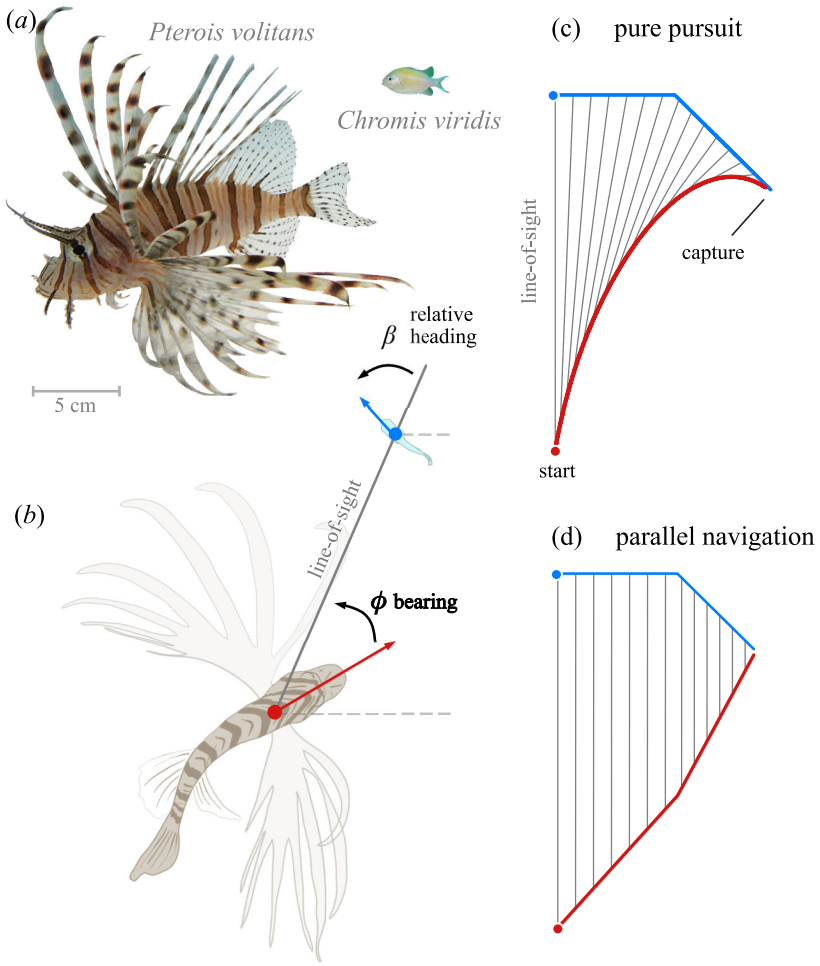

Figure 1.1: The kinematics of prey targeting. (*a*) Photos of the red lionfish (*Pterois volitans*) and prey fish (*Chromis viridis*), shown from a lateral perspective, scaled to mean total fish length. (*b*) The heading of the predator (red) and prey (blue) may depend on the line-of-sight (gray line), the predator's bearing (ϕ), and the prey's relative heading (β). (*c*–*d*) Trajectories of predators (red curves) target prey (blue curves) by either (*c*) 'pure pursuit' or (*d*) 'parallel navigation'. The two sets of trajectories are predicted from common starting positions (filled circles), with the line-of-sight (gray lines) drawn at an even interval. (*c*) Deviated pursuit is characterized by a predator maintaining a near-zero bearing. (*d*) Parallel navigation yields a non-zero bearing to direct the predator toward the point of interception with the prey.

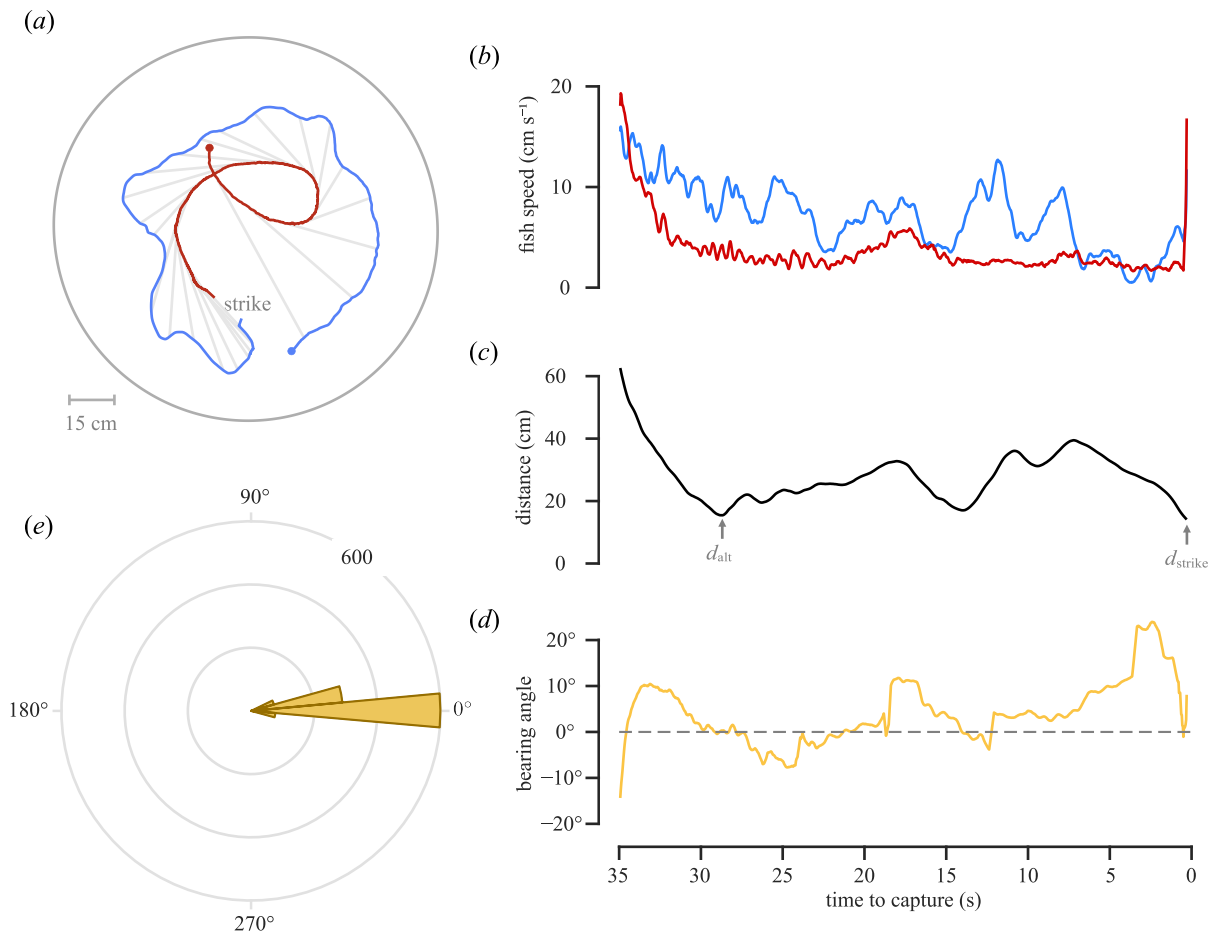

Figure 1.2: Representative kinematics from a single experiment. (*a*) Trajectories of lionfish (red curve) and prey (*C. viridis*, blue curve) in the final moments before capture (starting at filled circles) in a cylindrical tank (gray circle), with the line-of-sight (grey lines) drawn at a regular interval (1.4 s). (*b*–*d*) Kinematic variables are shown for the same period, including the (*b*) speed, (*c*) distance between the center of area of the animals, and the bearing (*d*) with respect to time and (*e*) in a polar histogram. (*c*) The distance at the time of the strike (d_{strike}) and the alternative minimum distance (d_{alt}), the next-closest distance achieved, are annotated in the plot.

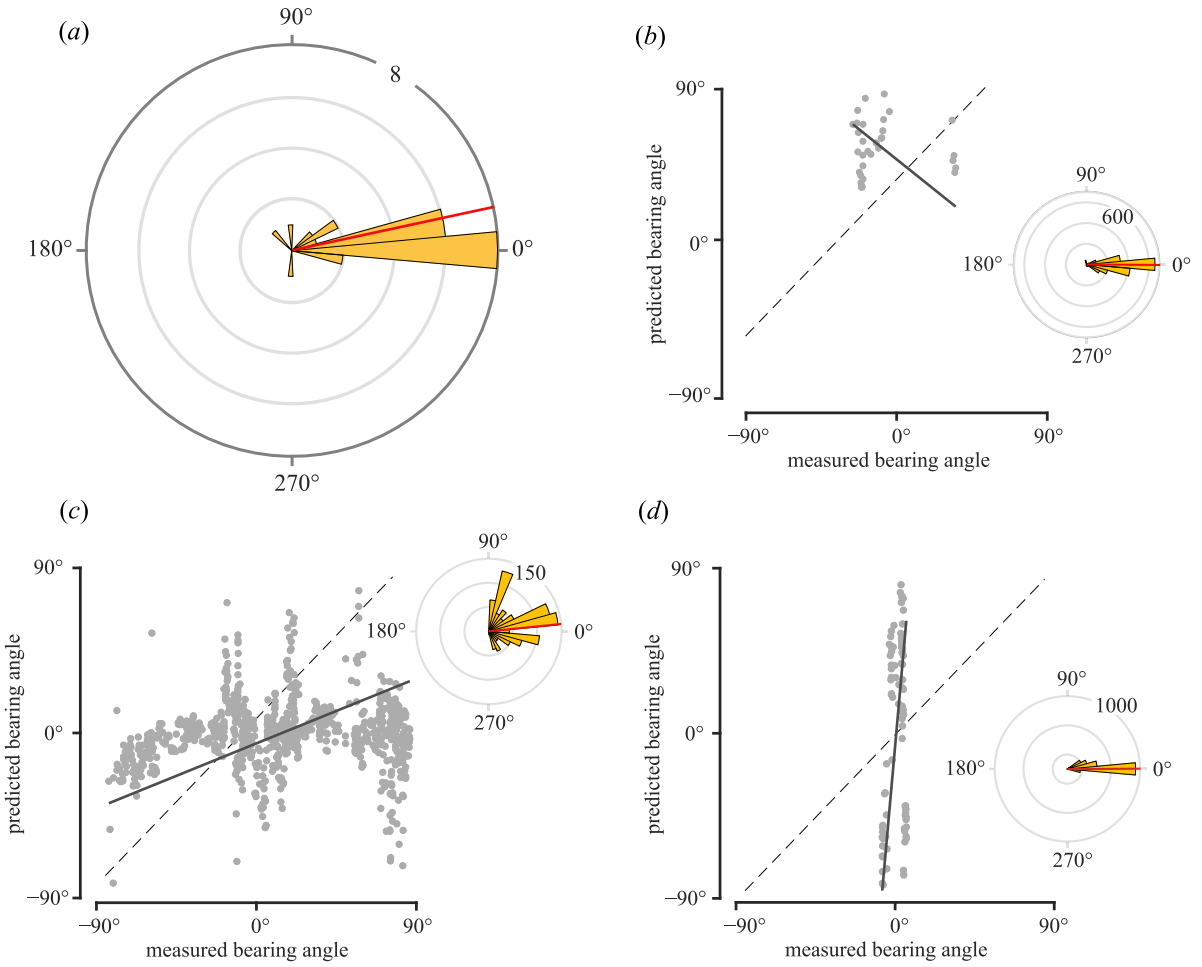

Figure 1.3: The kinematics of targeting by lionfish. (*a*) The circular mean bearings from all experiments are depicted in a polar histogram (counts). The total circular mean bearing (red line, $10° \pm 17.4°$ 95% CI, $n = 23$) was not significantly different from zero ($p < 0.05$, circular equivalent of a one-sample t-test with specified mean direction). (*b–d*) Representative regression analyses of pursuit strategy from three experiments, with the predator's measured bearing plotted against the calculated predicted bearing angles for parallel navigation. Deviations of the best fit by least squares (solid line) from the line of unity (dashed line) indicate that the measured bearing is not characterized by parallel navigation. None of the experiments analyzed with the regression analyses returned 95% confidence intervals that included the slope of unity ($n = 23$). The inset polar plots depict counts of measured bearing with a circular mean (red line).

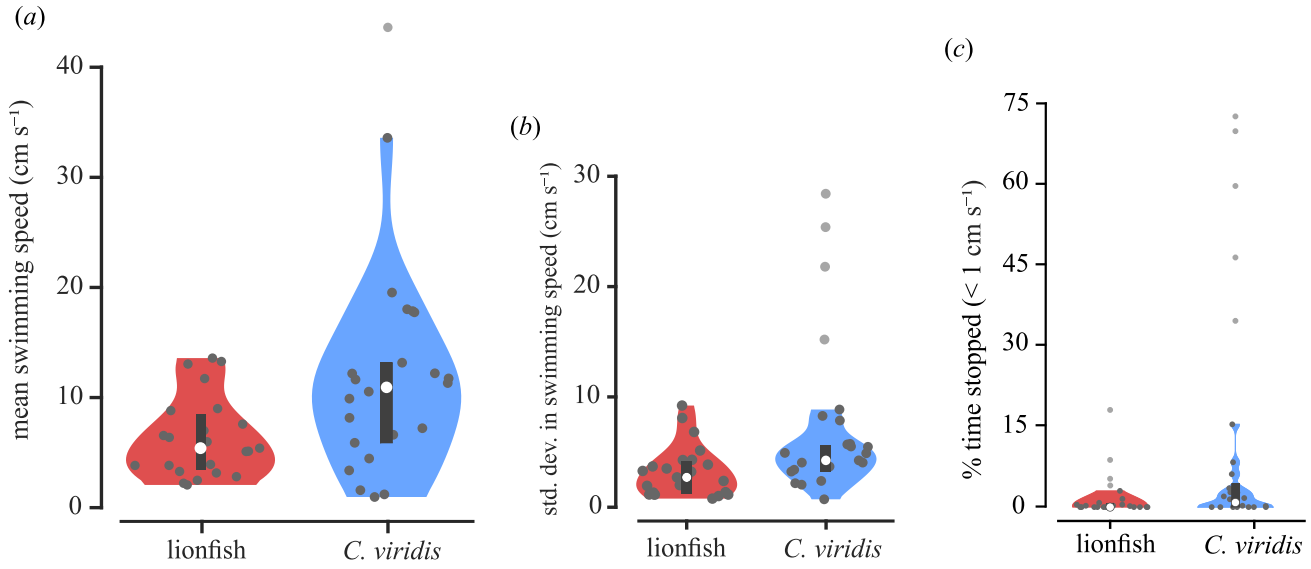

Figure 1.4: The speed and intermittency of predator (in red) and prey (in blue). (*a*–*b*) Speed data are depicted with violin plots (kernel density estimate of probability density function (PDF)). Inset boxplots depict the median value (white circle) and the boundaries of each box depicting the first and third quartiles (outliers are shown with light gray circles). The mean values from each experiment (dark gray circles) for the lionfish (red) and their prey (blue) are overlaid on the violin plot. The prey were about (*a*) twice as fast as lionfish ($n = 23$, $p = 0.02$, Wilcoxon rank sum test), with (*b*) a comparable standard deviation. (*c*) Summary of the proportion of time spent at near-zero swimming velocity (< 0.01 cm s^{-1}). Lionfish spent a much smaller proportion of time swimming at a near-zero velocity compared to prey ($n = 23$, $p = 0.008$, Wilcoxon sign rank test).

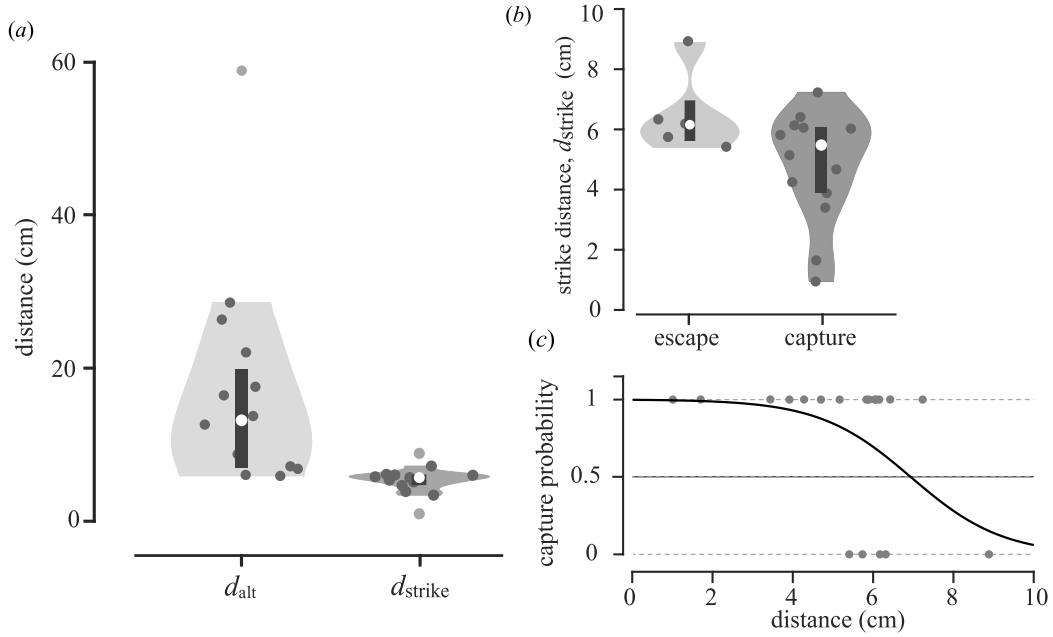

Figure 1.5: The distance between the prey and predator's rostrum at the strike. (a) Violin plots (as in figure 1.4) depict the alternative minimum-distance (d_{alt}, light gray) and the strike distance (d_{strike}, dark gray, $n = 13$). d_{strike} was significantly smaller than corresponding d_{alt} ($p < 0.001$, Wilcoxon sign rank test). (b) The strike distance of successful strikes (dark gray, $n = 5$) was on average, smaller than unsuccessful strikes (light gray, $n = 14$,). (c) The capture probability of strikes are shown as a function of strike distance for successful (value of 1) and unsuccessful (value of 0) strikes with a binomial logistic regression (black curve, $n = 19$) fit to the measurements.

Chapter 2

The evasion behavior of prey during encounters with devil lionfish (*Pterois miles*)

2.1 Abstract

Locomotion governs predator-prey interactions for a broad diversity of animals. Despite its importance, it remains unclear to what extent differences in locomotor behavior affect predation. The aim of the present study was to test the effects of variation in the avoidance locomotion of fish prey on their interactions with devil lionfish (*Pterois miles*). We selected four diverse prey species that differed in their locomotor strategy, from the continuous swimming of silversides (*Atherina* sp.), to the sea bream (*Sparus auratus*), which spent nearly half of the duration of experiments in a motionless state, with chromis (*Chromis viridis*) and mullet (*Mugil cephalus*) offering intermediate levels of spontaneous activity. Despite contrasting locomotor behaviors, the duration of the experiments and probability of capture

did not significantly differ between prey species. The devil lionfish targeted all prey with a strategy of pure pursuit and a conserved speed. These results challenge conventional thinking about the role of locomotion in mediating predator-prey interactions and offers insight into the devastating capacity of devil lionfish as invasive predators.

2.2 Introduction

Predation is largely determined by the locomotion of both predator and prey in a diversity of species. Contrasting patterns of prey avoidance reflect differences in vigilance, risk assessment, and past exposure to threats that may differentially affect the success or vulnerability to a predator [2, 8, 32, 1]. As they approach and attempt to capture the prey, predator may respond to variation in prey locomotion, in a manner reflected by their own physiology. Although the possibility of predators differentially responding to prey are broadly accepted [19], few studies have tested whether natural variation in swimming behavior among prey species affects their interactions with predators. The present study therefore aimed to test whether prey with differences in avoidance locomotion differ in the duration and outcome of their interactions with predators. Specifically, we measured the kinematics of interactions between individual devil lionfish (*Pterois miles*) and four different prey fishes with contrasting locomotor strategies and exposure to predators.

The targeting strategy of predators can be explored with kinematic measurements of predator and prey as they interact. A predator that heads directly toward the prey's instantaneous position is an example of a strategy known as 'pure pursuit' [79, 51, 65]. Pure pursuit has been observed in some flying insects [95, 56] and bats pursuing slow targets [15]. This form of targeting generates a curvilinear trajectory and is a specific example of a more general case where the predator attempts to maintain a particular bearing through time, which is called 'deviated pursuit' [79]. A time-optimal approach to prey capture follows a straight path to the point of interception, which may be achieved by a strategy known as 'parallel navigation' and is characterized by the line-of-sight maintaining its orientation in the global frame of reference. In an earlier study, we found that red lionfish (*Pterois volitans*) employ a persistent pure-pursuit strategy [73] with a single prey species. The present study evaluated whether a sister species, the devil lionfish (*Pterois miles*), retains this same strategy when

presented with a variety of prey species. This study aims to evaluate the influence of prey locomotor behavior on the pursuit strategy of lionfish.

Avoidance and evasive locomotion can enable prey to survive encounters with predators. Such antipredator behavior requires the recognition of the predator as a threat, which may be a challenge for prey exposed to a novel species. The 'naïve prey hypothesis' posits that the success of invasive predators may be attributed to the failure of prey to recognize the threat offered by an introduced species [80]. This hypothesis has been considered with red lionfish in comparisons between prey species from both their native Indo-Pacific and introduced Western Atlantic ocean regions [59, 57, 4]. Despite lionfish being invasive to the Western Atlantic Ocean, some native Atlantic prey species (damselfish and gobies) responded to lionfish with assessment and anti-predator displays that are normally employed with native Atlantic predators [54, 58]. In contrast, some Atlantic reef fishes have been shown to fail to responded to the lionfish as a predator [12]. Similar results have been obtained for Mediterranean reef fishes with devil lionfish [59, 25], which offers additional support for the naïve prey hypothesis. The discrepancies among studies may be partially attributed to differences in the metrics of observed behavior and a common focus on prey that are physically separated from the lionfish. The present study offers a novel contribution in approach by considering the free-swimming behavior of a single predator and single prey and the effects that locomotor behaviors have on capture probability and the duration of the encounter.

The devil lionfish were collected from reef habitats just a few kilometers away from where our native prey species were also collected. To explore the influence of predator-prey kinematics on the outcome of interactions, we first examined whether devil lionfish employed the same pursuit strategy as the previously-studied red lionfish [73] and whether this strategy was dependent on the prey's behavior. Secondly, we examined the locomotor performance of prey as they interacted with devil lionfish and documented its effects on the success of the

behavior. We chose four prey species for the present investigation that inhabit a variety of ecological habitats, some of which are shared with the devil lionfish. These lionfish actively hunt prey in the midwater, in and around reefs, and along the seafloor [62].

The chromis (*Chromis viridis*) is a common reef-associated damselfish in tropical marine habitats, from the Red Sea to the Indian and Pacific Ocean basins (figure 2.1) [36]. This species is known to be preyed upon by red lionfish in the Pacific Ocean and, given their abundance, are likely a common prey of the devil lionfish [36, 62]. Small groups of chromis can be found hovering above coral heads and will dart back into the reef complex when disturbed. Silversides (*Atherina* sp.) are a common midwater prey of devil lionfish [62] and they create large schools that disperse after dark (pers. observ.). We collected chromis and silversides from habitats where devil lionfish are routinely observed and we therefore considered them to be native species and not naïve. Mullet (*Mugil cephalus*) are found nearly worldwide in tropical to temperate costal waters, including the Red Sea. This species is popular for aquaculture and is a crucial food source for many piscivorous predators [93]. Because we sourced juvenile mullet from an aquaculture facility, we considered this species to be native, but naïve, to devil lionfish. Finally, we presented devil lionfish with a non-native, naïve prey choice, the gilthead sea bream (*Sparus aurata*). Sea bream are an abundant coastal species in the Mediterranean Sea, where juveniles recruit on rocky reefs or sea grass beds, and are a valued species in recreational, commercial, and aquaculture fisheries [63, 30]. Like the mullet, the sea bream were raised in a local aquaculture facility and thus were generations removed from any kind of predator pressure.

2.3 Material and methods

2.3.1 Animal husbandry

Experiments were conducted at the Interuniversity Institute for Marine Sciences (IUI) in Eilat, Isreal between October 11 and November 4, 2018. The animals were obtained through a combination of field collection and purchase through the aquarium trade. Red sea chromis (*C. viridis*, $n = 9$, mean total length, TL $= 4.4 \pm 0.3$ cm) and silversides (*Atherina* sp., $n = 4$, TL $= 5.5 \pm 0.1$ cm) were collected on SCUBA and by free diving with hand nets from reefs local to the IUI. The fish were fed an enriched diet daily and housed in a 100 L tank with flow-through seawater. Seabream (*S. auratus*, $n = 10$, mean TL $= 5.2 \pm 1$ cm) and mullet (*M. cephalus*, $n = 7$, TL $= 3 \pm 0.5$ cm) were sourced from a local aquaculture facility and held in recirculating 100 L aquaria, refreshed regularly with seawater. Devil lionfish (*P. miles*, $n = 4$, TL $= 23.4 \pm 8.3$ cm) were collected with hand nets (from a depth of ~ 30 m) and housed together in a large outdoor tank (~ 1000 L) with flow-through seawater (26°C, 40.5 ppt; 60m^3 per hr). Throughout our predation experiments, the devil lionfish were permitted to feed on a maximum of two prey in an 18 hr period and were not given supplemental feedings to keep them motivated for prey pursuit.

2.3.2 Behavioral experiments

Our experiments entailed video-recording the behavioral interactions between individual devil lionfish and prey fish. Experiments were conducted in a circular arena ($\varnothing \sim 1.6$ m, with water depth of 0.3 m) and filmed from above with a DSLR camera (1080×1920 at 60 fps, Sony Alpha, A7SIII or A7RIII, Sony Electronics Inc., San Diego, CA, USA) using an external recorder (Atomos Ninja Flame, ATOMOS Global Pty Ltd, Los Angeles, CA, USA). The arena was illuminated from above with fluorescent and LED lights. A fine-mesh barrier

was suspended just below the water's surface to dissipate surface ripples created by the fins of the devil lionfish. The prey fish were introduced to the arena and allowed to acclimate undisturbed for 1 hr before the devil lionfish was introduced and the recording began. The interactions were permitted for up to 1 hr, if the prey failed to be captured by the devil lionfish. Prey fish that survived the experiments were not reused.

We used kinematic measurements to characterize the targeting behavior of devil lionfish and the avoidance behavior of prey fish. These measurements consistent of tracking the body position of both the predator and prey fish in the 5 min leading up to the moment when the predator came closest to the prey. In the majority of experiments, the closest distance was achieved when the predator attempted a predatory strike towards the prey. We extracted the position of each fish using semi-automated tracking software (in MATLAB, v. 2019b, MathWorks, Natick, MA, USA) that was developed previously [73]. This software uses grayscale thresholding for instance segmentation to locate the centroid of each animal's center-of-area, but requires manual tracking of the prey for video frames with poor contrast. After smoothing positional measurements with a moving average (0.33 s), we discretely calculated the speed, distance, and heading (θ) from the trajectory of each animal. We found the proportion of time that each fish spent at a near-zero velocity (< 0.005 cm s^{-1}) as a metric of intermittent swimming.

To relate fish movements to behavioral strategy, we calculated the orientation of predator and prey relative to the line-of-sight, which is the axis drawn between the position of the prey and rostrum of the predator (figure **??***b*). A prey's relative heading was calculated as the orientation of the prey relative to the predator's position, as follows:

$$\beta = \tan^{-1}\left(\frac{\sin\left(\alpha - \theta_{\text{prey}}\right)}{\cos\left(\alpha - \theta_{\text{prey}}\right)}\right), \tag{2.1}$$

where θ_{prey} is the prey's heading and α is the angle of the line-of-sight relative to the inertial frame of reference. The bearing angle (ϕ) was calculated as follows:

$$\phi = \text{sgn}(\dot{\theta}_{\text{pred}}) \tan^{-1}\left(\frac{\sin(\alpha - \theta_{\text{pred}})}{\cos(\alpha - \theta_{\text{pred}})}\right), \tag{2.2}$$

where θ_{pred} is the predator's heading and $\dot{\theta}_{\text{pred}}$ is its rate of change. The sign of $\dot{\theta}_{\text{pred}}$ indicates when the heading is directed to the left ($\text{sgn}(\dot{\theta}_{\text{pred}}) = 1$) or right ($\text{sgn}(\dot{\theta}_{\text{pred}}) = -1$).

To test whether devil lionfish alternatively moved with parallel navigation, we compared bearing measurements against the bearing predicted (ϕ_{para}) by the following equation [79]:

$$\phi_{\text{para}} = \sin^{-1}\left(\frac{s_{\text{e}} \sin\beta}{s_{\text{p}}}\right), \tag{2.3}$$

where s_{e} and s_{p} are respectively the speed of the prey and predator. This calculation was only possible for during periods when the prey was either slower or directed towards the predator.

2.3.3 Statistical analysis

Our analysis included non-parametric statistical tests, due to many measurements' failure to conform to a normal distribution [94]. Normal distributions were assessed with a One-sample Kolmogorov-Smirnov tests [94]. Relationships between independent variables, such as predator and prey speed, were evaluated using a Wilcoxon rank sum test. We used the Kruskal-Wallis test, which is a non-parametric equivalent of a one-way ANOVA, to analyze mean measures of kinematic data between individual predators or individual prey species. Angular data were evaluated with circular statistics, specifically employing the 'CircStat' toolbox available for use in MATLAB [11]. Predicted bearing angles (determined using 2.3) were evaluated against measured bearing angles using a Model II linear regression (reduced

major axis regression). This method evaluates variables that are subject to measurement error, without assuming dependence, such as a measurement and a prediction.

2.4 Results

2.4.1 The predatory behavior of devil lionfish

Devil lionfish were effective at targeting prey in our experiments. These predators attempted strikes in in the majority of all encounters with seabream (90%) , mullet (90%), and silversides (90%). Chromis were the most evasive prey species and devil lionfish attempted a strike in only 5 out of 9 individuals, successfully capturing 3. In the remaining two attempted strikes, *C. viridis* escaped above the submerged, near-transparent, fine-mesh lid prior to a strike. Devil lionfish still attempted to strike but we consider the outcome to be undetermined. Predator and prey encounters spanned from 3 s to just over 1 hr (mean duration $\pm$ 1 SD $= 12.7 \pm 20.2$ min), but the average encounter duration did not differ significantly between prey species ($p = 0.62$, $n = 4$), nor was there any effect of a particular lionfish individual ($p = 0.62$, Kruskall-Wallis test, $n = 4$).

Predator targeting strategy can be tested by examining the relationships between a predator's heading and the bearing angle (figure 2.1). Devil lionfish pursued prey with a near-zero bearing, a strategy that was conserved across all prey species ($p = 0.63$, $n = 30$, circular one-factor ANOVA, figure 2.3*a*–*e*). We applied a reduced-major-axis regression to each encounter that tested whether variation in bearing angle within individual encounters were explained by values predicted for parallel navigation. We found that this relationship between predicted and measured bearing angle was significantly different from unity in all 30 experiments ($p < 0.05$, reduced-major-axis regression, figure 2.3*f*). Thus, regardless of

prey type, devil lionfish maintained a strategy of pure pursuit, with variation that was not explained by parallel navigation.

The suction-feeding strike of lionfish is a critical facet of their effectiveness as predators. Devil lionfish succeeded in capturing prey at distances between 1 and 14 cm from the mouth. The average strike distance was not significant different between prey species (figure 2.4*d*) and only varied between the two predators with the largest and smallest strike distances (devil lionfish '1' and '4', figure 2.4*c*). Devil lionfish '1' attempted only two strikes, both at with the same prey species (sea bream) and at close distance in instances where the prey spent a large proportion of the experiments paused. We found little difference in the pursuit strategy of individual devil lionfish, regardless of predator size ($p = 0.032$, $n = 4$). The consistency of lionfish predatory behavior indicates a conserved pursuit strategy where variation in outcome is largely determined by the behavior of prey.

2.4.2 Swimming behavior

The devil lionfish were quick to identify a potential target and would immediately begin advancing toward the prey at the outset of the experiments. They approached prey at a speed (8.5 ± 11 cm s^{-1}) that was consistent among individuals ($p = 0.77$, $n = 30$, Kruskall-Wallis test, figure 2.4*a*) and did not differ between prey species ($p = 0.77$, $n = 4$, Kruskall-Wallis test, figure 2.4*b*). The prey species differed in their behavioral response to the devil lionfish. The mean swimming speed of seabream, mullet, chromis, and silversides was similar to that of the devil lionfish ($p = 0.11$, $p = 0.30$, $p = 0.07$, $p = 0.37$, $n = 10$, 7, 9, and 4, respectively) but this metric alone obscures the individual variation of prey swimming behavior (figure 2.6*a*–*d*). We explored the swimming capacity of devil lionfish, which we defined as the 90$^{\text{th}}$ quantile of speed measurements, and the range between the 90$^{\text{th}}$ and 10$^{\text{th}}$ quantiles (figure 2.6*a*–*d*). The seabream were on average, slower than the devil lionfish but were capable

of exceeding the speed capacity of the predator (figure 2.4*a*). The silversides had a mean swimming speed similar to that of the devil lionfish but maintained a slightly greater capacity and range for swimming velocity (figure 2.6*d*). The mullet and chromis were nearly twice as fast as the devil lionfish (7 ± 2.6 cm s^{-1}) in mean values, with both species exhibiting a large capacity for speed compared to the predator ($p = 0.05$ and $p = 0.04$, $n = 7$, respectively, Wilcoxon rank sum test, figure 2.6*b,c*).

A major difference between the devil lionfish and prey was the degree to which they would pause their swimming. We measured the proportion of time that the fish remained nearly stationary (i.e., < 0.005 cm s^{-1}, figure 2.7*a–b*). Seabream ($42 \pm 38.4\%$) and mullet ($42.1 \pm 24\%$) spent nearly half of the time motionless, while the devil lionfish they encountered were in nearly perpetual motion (0.1%), a difference that was statistically significant ($p = 0.01$, $n = 10$, $p = 0.02$, $n = 7$, figure 2.7*a,b*). Chromis and the devil lionfish they interacted with spent a similar proportion of time stopped ($16.2 \pm 27.7\%$ and $< 1\%$, $p = 0.19$, $n = 9$, figure 2.7*c*) In contrast, the silversides and the devil lionfish they encounted spend a very little proportion ($< 1\%$) of the time paused (figure 2.6*d*). Individual devil lionfish were similar ($< 15\%$, $p = 0.07$, $n = 4$, Kruskall-Wallis test) in their pausing behavior.

2.5 Proximity-dependent effects on pursuit and evasion

We evaluated whether swimming kinematics of animal changed as the devil lionfish closed the distance to their prey. As established above, the bearing was not significantly different from zero (figure 2.3), but we observed a greater degree of variation in the predators bearing at greater distance (figure 2.8*a–d*). This variation may largely be attributed to the reorientation of the predator while searching for the prey. The relative heading of the prey indicates their

direction of swimming in relation to the line-of-sight (figure 2.1). We found that prey tended to evade devil lionfish at a right angle to the line of sight ($p = 0.57$, $n = 30$, circular equivalent to the Kruskal-Wallis test for median direction, figure 2.8*i*), with neither a clear difference between species, nor differences that correlated with distance (figure 2.8*e–h*). We found that the speed of prey tended to approach that of the predator as the distance between the animals approached zero. We calculated the difference in speed between predator and prey, such that values below zero indicated when the prey was faster than the predator (figure 2.9*a–d*). These measurements showed that the speed of predator and prey became more similar when at close proximity. This pattern aligns with the tendency of all prey to spend a smaller proportion of their time stopped when the predator was within close proximity.

2.6 Discussion

Our kinematic measurements addressed how predator-prey interactions differ among prey species with a common predator, the devil lionfish. We considered whether the devil lionfish employ different targeting strategies for different prey. Our measurements of prey locomotor behavior revealed how species differed in their temporal patterns of locomotor behavior (figure 2.6). The behavior of both predator and prey collectively yielded experiments where the duration of the interaction and probability of prey capture that were similar across all prey species.

We tested how devil lionfish targeted prey and whether they vary their strategy in response to species-specific behavior. Given the differences in motion by the prey (figures 2.5 and 2.6), it is reasonable to predict that targeting behavior by lionfish could vary as well. However, we found that devil lionfish maintained a bearing close to zero (figure 2.3*a-d*) for all species, with deviation from that value only at relatively large distances (figure 2.8*a-d*). This pattern is consistent with a pure-pursuit strategy and we found no support for parallel navigation

(figure 2.3*f*). In addition, the devil lionfish maintained a consistent swimming speed across individuals, irrespective of the prey species (figure 2.4*c-d*). We therefore failed to find any differences in strategy when devil lionfish preyed upon different species, like what has been observed among aerial predators [51, 65, 95, 56, 15]. Pure-pursuit was previously discovered for a lionfish species of the same genus (*Pterois volitans* [73]) and bluefish were found to employ a similar strategy [60]. The generalist nature of lionfish, and their ability to forage in a variety of habitats [62, 23, 25] might indicate a plastic pursuit strategy, but it is instead possible that a single strategy may be sufficiently general to prey locomotor behavior. It is furthermore possible that pure pursuit is a targeting strategy that is general to fishes.

The consistency in predator behavior is perhaps surprising given the differences in prey behavior that we observed. These differences were most apparent in the extent to which swimming was intermittent. The silversides rarely stopped moving (figure 2.7*d*) and consequently exhibited a relatively low degree of temporal variation in acceleration. Although the sea bream achieved an indistinguishable difference in mean speed (figure 2.6), that species often did not swimming a large proportion of the time in our experiments (figure 2.7*a*). A lack of swimming may be due in part to a lack of conspecifics, as this species is tank-raised in population densities much higher than would be seen in a wild-caught animal, or a tendency to respond to a threat by freezing, which is a behavior where the prey ceases motion in response to a predator's appearance [19]. However, sea bream still regained the capacity to respond to the predator at close distances (figure 2.9*a,e*) suggesting a switch in avoidance strategy that may be distance-dependent. Mullet were also raised in high densities, but attained similar degree of intermittent swimming and mean speeds to that of chromis. Chromis maintained intermediate swimming speeds and only a few individuals spent a greater proportion of time stopped. Typically found foraging above coral heads, chromis are rapid swimmers that can inhabit areas of high current, but are dependent on the refuge of the coral complex [36, 75]. Despite the contrast in swimming behavior among prey species, the outcome of their interactions with devil lionfish were similar. Both the duration

of the interactions and probability of prey capture were indistinguishable between experiments that featured different prey species. These ultimate metrics of predation performance occurred despite the consistency in targeting behavior by devil lionfish, which suggests a lack of compensation by the predator for the differences in prey behavior.

The similarity in outcome across prey may be partially understood through the similarities among prey species, beyond the aforementioned mean speed of swimming. We incorporated the difference in fish speed in relation to the distance between animals. Although the species varied in swimming speed and in their degree of intermittent swimming, these differences reduced as the devil lionfish approached. In particular, we found that all species moved continuously (figure 2.9*e*) with a speed close to that of the devil lionfish (figure 2.9*a*-*d*) when the predator and prey were close to one-another. This suggests that prey recognize devil lion fish as a threat, yet generally fail to maintain their distance, regardless of their swimming abilities. Animals in multi-predator environments may have the capacity to avoid many threats [13], but the response of completely naïve species (e.g., seabream and mullet) may be attributed to the innate response of animals to avoid a looming stimulus, rather than a specific response to lionfish [61, 87, 28]. An additional similarity among species was the direction of swimming. All prey species tended to move in a direction that was perpendicular to the line-of-sight, irrespective to their distance from the devil lionfish (figure 2.8*e*-*i*). Therefore, prey responded to the devil lionfish in a similar manner, especially when close enough to permit a suction-feeding strike by the predator.

2.7 Summary

In summary, the interactions between devil lionfish and four diverse prey are generally similar, regardless of prey ecology and prior exposure to predators. The vast majority of these interactions ended in a successful prey capture, with a pursuit that transpired over a similar

period of time. These similarities in outcome occurred despite the prey moving intermittently to a variable degree and the devil lionfish varying little in their targeting strategy and swimming speed. Despite these differences in locomotor capacity among prey, all tended to approach a similar swimming speed to the devil lionfish at close distance and thus the interactions were similar. Therefore, prey appear to respond to devil lionfish in a similar manner, despite their otherwise distinct behavior. These results offer alternative hypothesis for the predatory success of both the red lionfish and the devil lionfish, in that the outcome of an interaction is less dependent upon the capacity of prey to respond and more on the robust nature of a slow persistent approach. This strategy is likely aided by the unique appearance of lionfish and the potential for their large pectoral fins to reduce the available space available for prey evasion.

2.8 Figures and tables

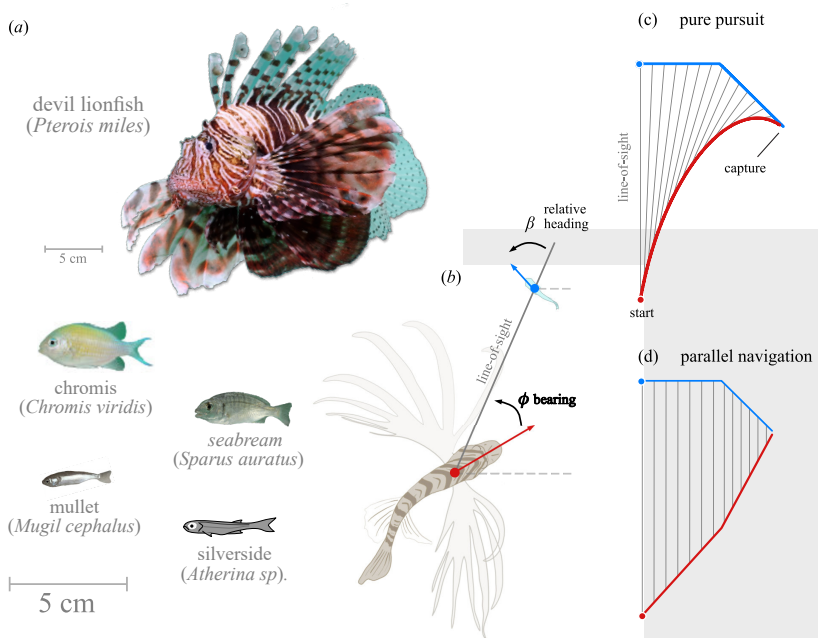

Figure 2.1: Study species and kinematic parameters. (*a*) The predator species, the devil lionfish (*Pterois miles*), and prey fishes, chromis, sea bream, mullet, silversides (sketch), shown from a lateral perspective, scaled to mean total length. (*b*) The heading of the predator (red) and prey (blue) may depend on the line-of-sight (gray line), the predator's bearing (ϕ), and the prey's relative heading (β). (*c–d*) Trajectories of predators (red curves) target prey (blue curves) by either (*c*) 'pure pursuit' or (*d*) 'parallel navigation' targeting strategies. The two sets of trajectories are predicted from common starting positions (filled circles), with the line-of-sight (gray lines) drawn at an even interval. (*c*) Pure pursuit is characterized by a predator maintaining a zero bearing. (*d*) Parallel navigation yields a non-zero bearing to direct the predator toward the point of interception with the prey.

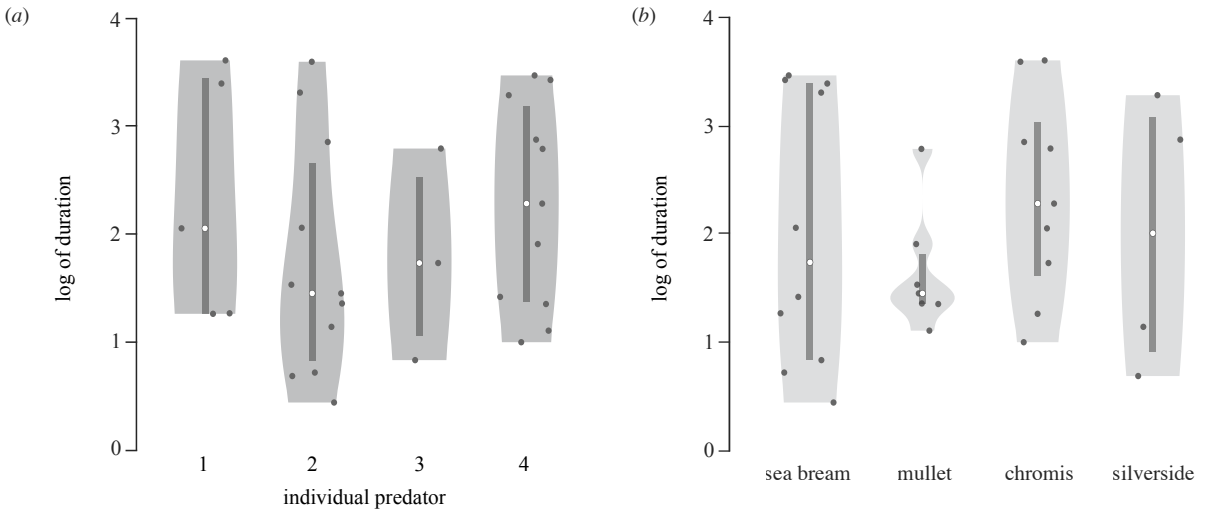

Figure 2.2: The duration of experiments. (a) The total duration of experiments (log10 transformed). Each measurement represents the time to a predatory strike, or a 1 hr duration, if no strike occurred. The individual duration measurements (gray circles) are displayed in seconds and transformed with a 10-base logarithm and grouped by the (a) individual predator and (b) the prey species. The distribution of values are visualized with violin plots that include kernel density estimate of the probability density function (shaded area) with inset boxplots (vertical line) with boundaries that depict the first and third quartiles with the median value highlighted (white circle).

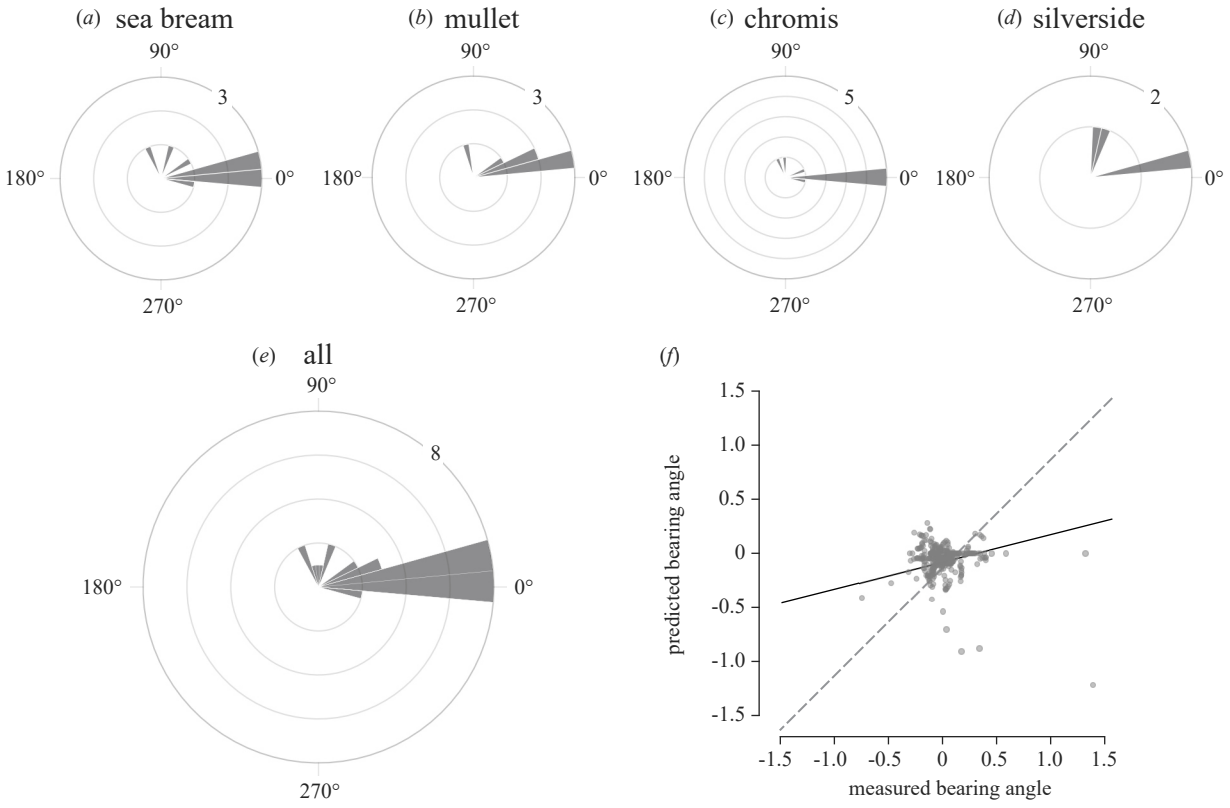

Figure 2.3: The predatory targeting behavior of devil lionfish. $(a–e)$ The mean bearing angle measured during encounters with each prey species was not statistically different from zero $(p < 0.05,\ n = 30)$. $(a–d)$ Individual counts of mean bearing angle for each prey species, (a) seabream, (b) mullet, (c) chromis, and (d) silversides. The mean bearing angle was indistinguishable between prey species. (c) A representative regression analyses of pursuit strategy from a devil lionfish and chromis, with the measured bearing plotted against the calculated predicted bearing angles for parallel navigation. Deviations of the best fit by least squares (solid line) from the line of unity (dashed gray line) indicate that the measured bearing is not characterized by parallel navigation. None of the experiments analyzed with the regression analyses returned 95% confidence intervals that included the slope of unity $(n = 30)$.

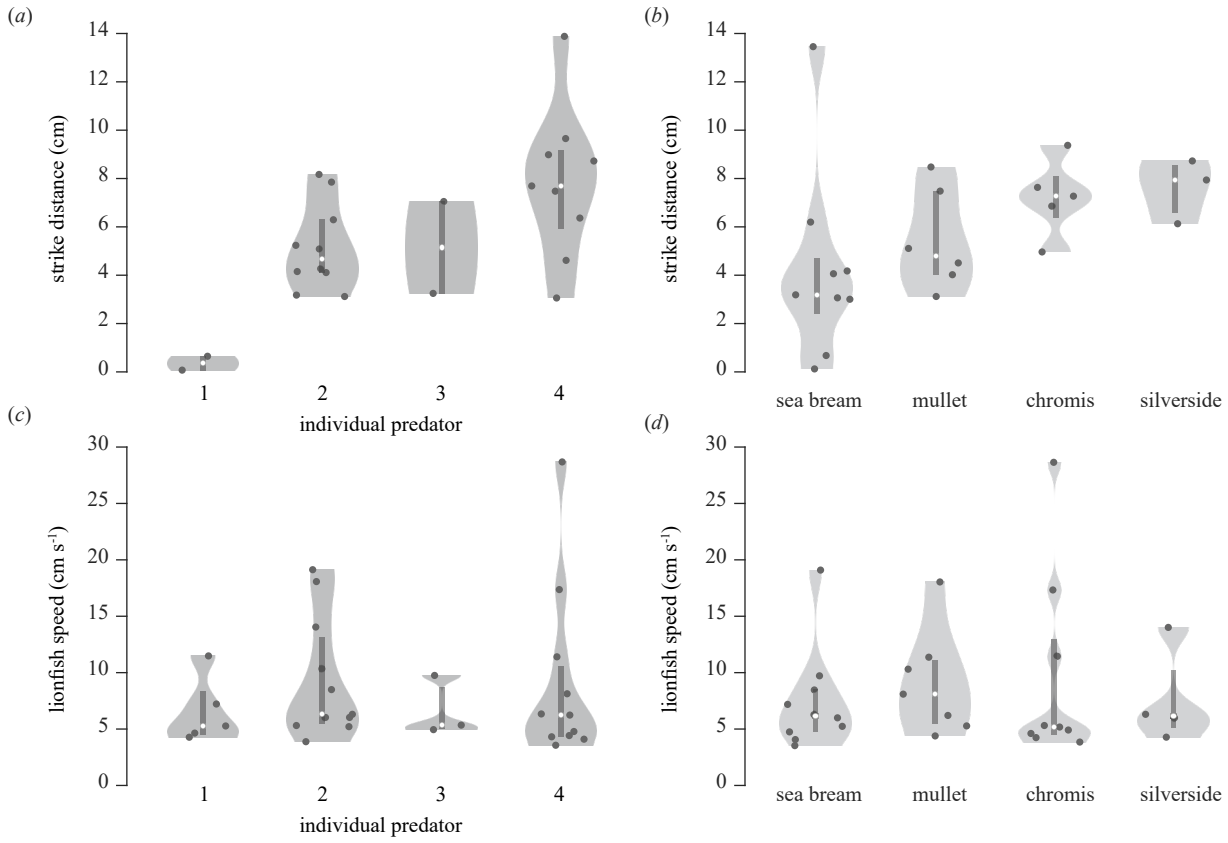

Figure 2.4: devil lionfish swimming speed and strike distance. The pursuit behavior of devil lionfish remained constant regardless of prey species, with very little variation between individual predators. (*a*–*b*) The strike distance of devil lionfish was conserved across individuals and across prey species. (*c*–*d*) devil lionfish exhibited little variation of swimming speed between individuals irregardless of prey species. The violin plots are described in the legend text for figure 2.2.

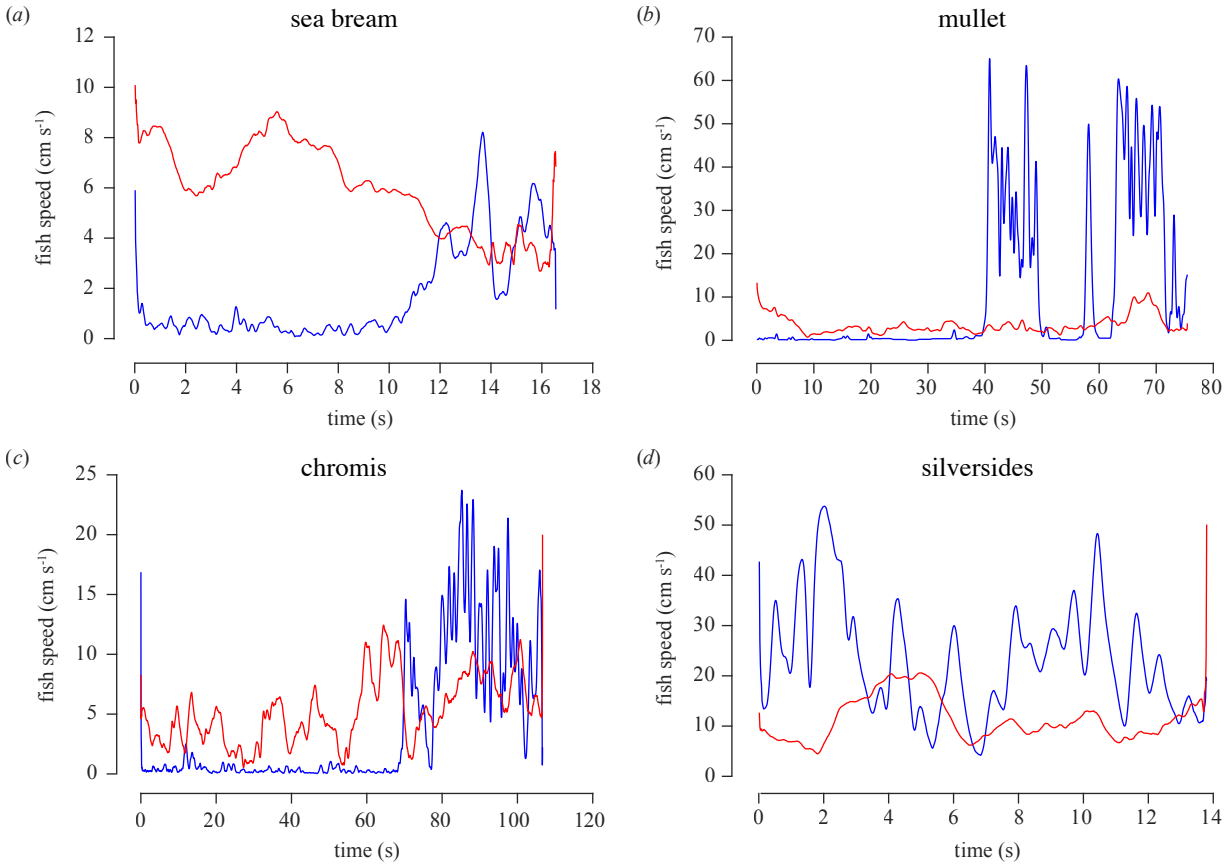

Figure 2.5: Representative time-series measurements of speed from experiments for each prey species. Values for the devil lionfish (red curves) and the prey (blue curves) are shown for (a) sea bream, (b) mullet, (c) chromis, and (d) silversides.

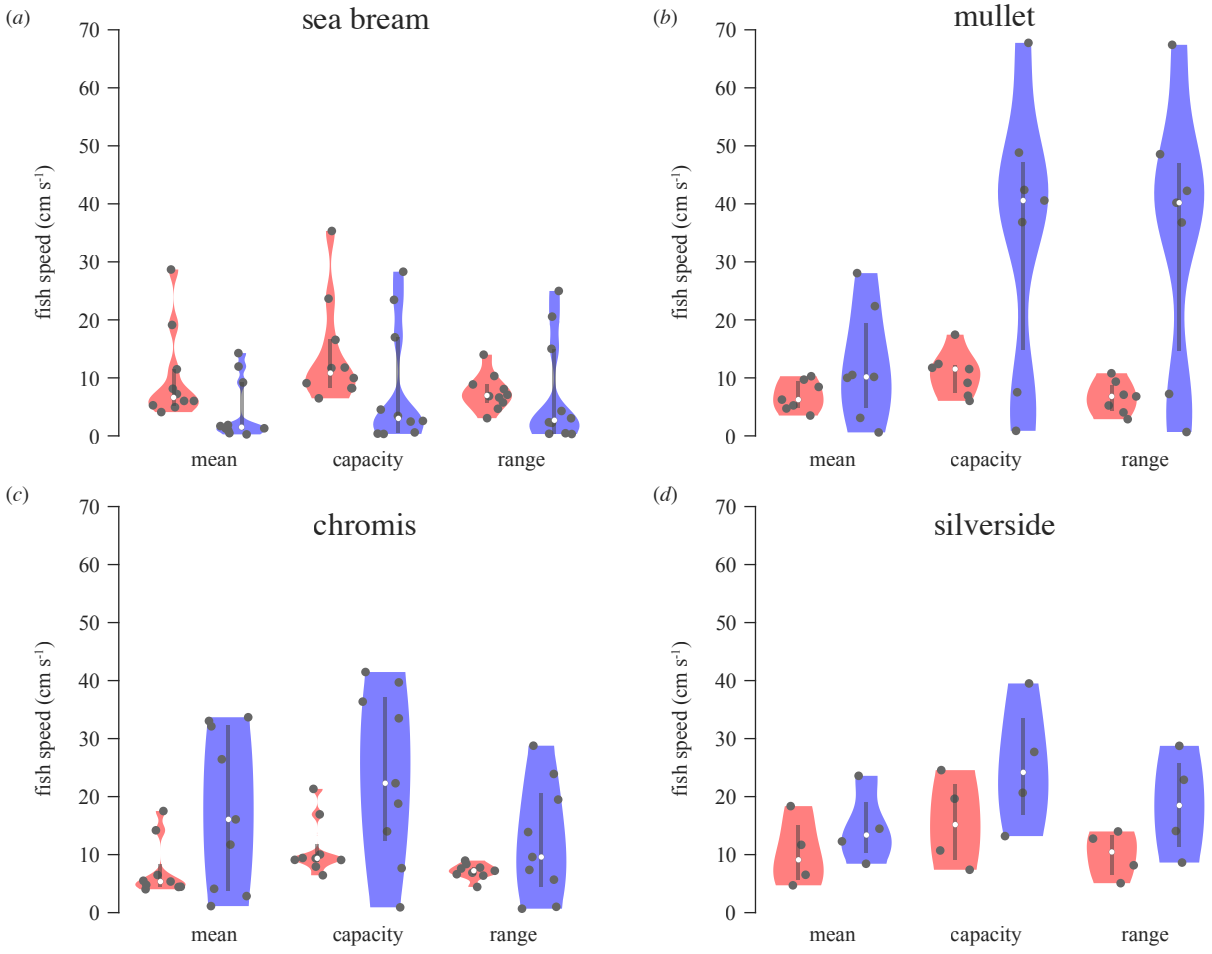

Figure 2.6: Descriptors of swimming speed for devil lionfish and prey. (a–d) Three metrics of speed (mean speed, capacity, and range) were used to asses the swimming behavior of devil lionfish during interactions with (a) seabream, (b) mullet, (c) chromis, and (d) silversides. The mean swimming speed of predator and prey between species groups was similar. Apart from seabream, prey generally maintained greater capacity for speed and a greater speed range. The violin plots are described in the legend text for figure 2.2.

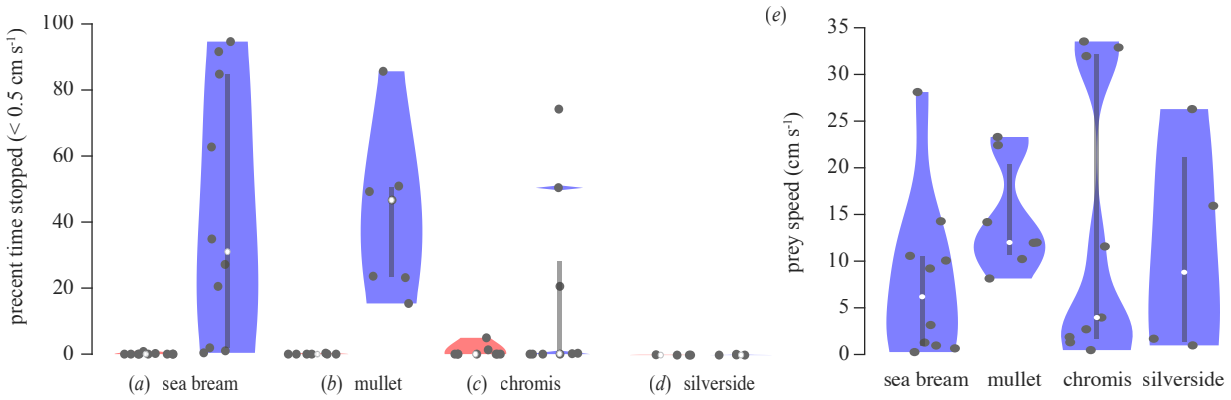

Figure 2.7: The proportion of time devil lionfish and prey spent swimming. Devil lionfish spent a very small proportion of time stopped relative to the prey, however between individuals within an experiment, the difference was not always significant. (a,b) Seabream and mullet spent greater periods of time at near zero speeds, relative to the devil lionfish they encountered. (c) chromis and devil lionfish spent similar proportions of time stopped, however the variation was greater among the prey. (d) Silversides and the devil lionfish they interacted with spent almost the entire interaction swimming. The violin plots are described in the legend text for figure 2.2.

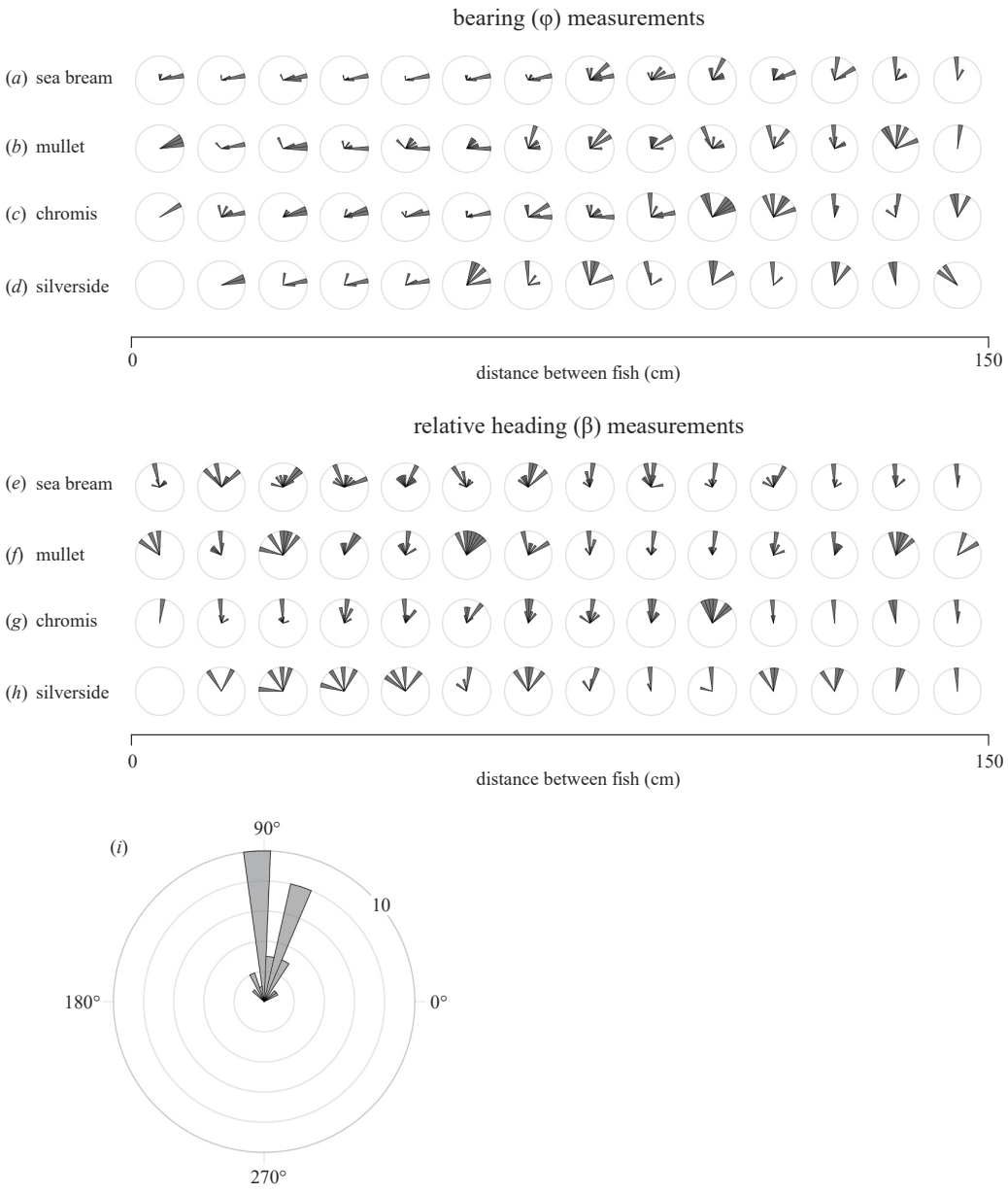

Figure 2.8: The relationship between fish distance and the bearing and relative heading angles of devil lionfish and prey. *a–c* Polarhistograms (counts) of the absolute value of the mean devil lionfish bearing angle for a given proximity. (*e–h*) Polarhistograms (counts) for the absolute value of the mean relative heading of each prey species. *i* The absolute value of pooled mean relative heading angles from all prey species is depicted in a polarhistogram (counts). All species shared a common mean relative heading angle (abs. value) that was similar to 90°. (*a–h*) Each circle within a row represents the average bearing from interactions within individual species. Columns correspond to specific distances (grouped by 10 cm bins). Distance bins increase in value from left to right. The angular coordinates for individual polarhistograms are identical to (*i*) (*a–c*) As the distance between predator and prey reduces, devil lionfish bearing concentrated heavily arount a zero bearing angle. (*e–h*) There was very little influence of distance on the relative heading of the prey, regardless of prey type.

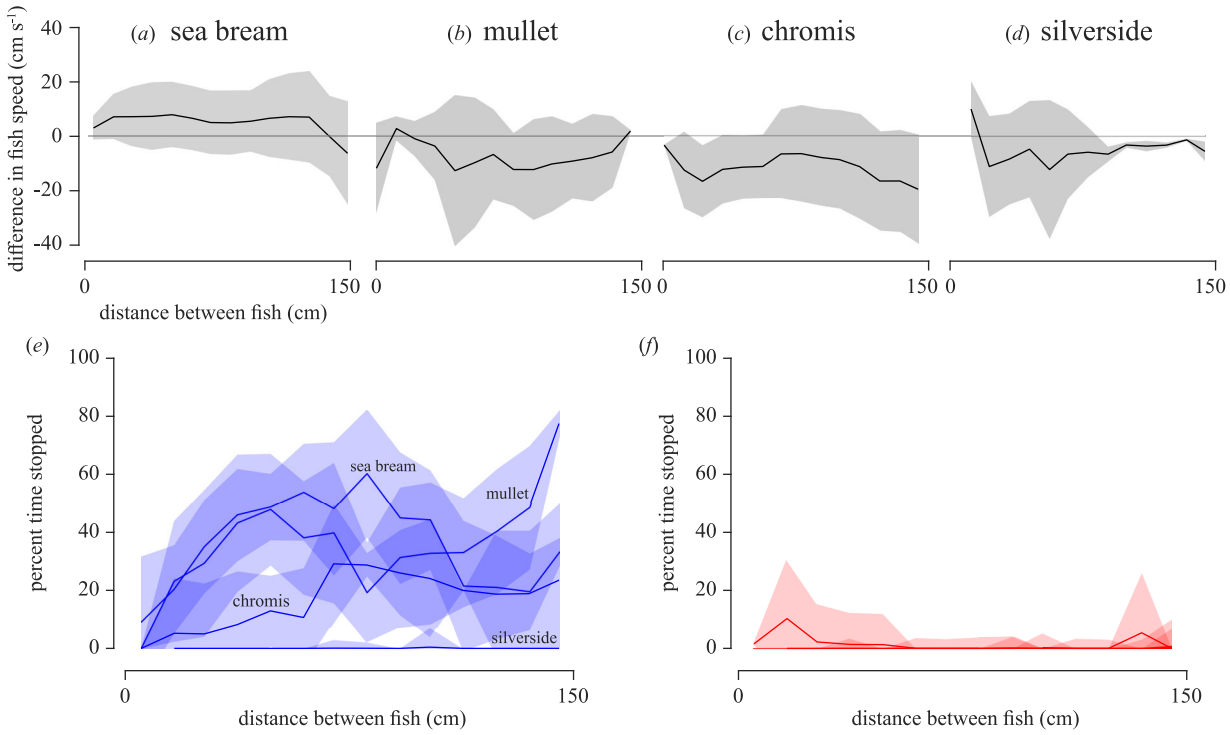

Figure 2.9: Metrics of the swimming behavior of devil lionfish and prey as a function of distance. (*a–d*) The relative mean speed difference between devil lionfish and prey, binned by distance is depicted by the black lines. The standard deviation is depicted with a grey shadow. The horizontal grey line depicts a speed difference of zero, indicating the speed of the predator and prey is matched. Speed difference values greater than zero represent a relatively slower prey, while speed difference values less than zero represent a relatively faster prey. The relative speed varied with distance but generally approached, or crossed zero for all prey species as the distance declined. (*e–f*) The average proportion of time spent at a near zero velocity for the (*e*) prey (blue lines) and (*f*) devil lionfish (red lines) were determined across bin distances. The standard deviation is depicted with a colored shadow. (*e*) All prey (except silversides, blue line closest to zero) spent a greater proportion of time swimming at the furthest distance bins. The proportion of time stopped, began to approach zero with increasing proximity to the predator. (*f*) Devil lionfish spent nearly all of every experiment swimming, however, in some instances where the distance between lionfish and prey was small, the devil lionfish paused more frequently.

Chapter 3

Modeling as a tool for uncoupling predator-prey interactions

3.1 Abstract

The outcome of predator-prey interactions depends on how the animals respond to one-another. Such interactions are defined by a myriad array of traits in sensing, neural processing, and biomechanics. The coupled nature of these behavioral interactions challenge the ability to resolve what aspects of performance matter to whether prey are captured. To address this challenge, we developed a 2D agent-based mathematical model for a fish predator and an individual prey fish enclosed within a circular arena. We parameterized and tested the predictions of this model with previous experimental measurements of the trajectories of red lionfish (*Pterois volitans*) as they preyed upon a smaller reef fish (*Chromis viridis*). Lionfish successfully capture a diversity of prey types, including prey with a greater capacity for speed and maneuverability. Consistent with experimental observations, the predator controlled its heading to target the prey with a pure-pursuit strategy and the prey moved

with intermittent bouts of swimming. Based on these behavioral rules, we performed numerical simulations to predict the trajectories of predator and prey, until the predator closed within sufficient distance for a suction feeding strike. These simulations were performed with a Monte-Carlo approach where some of the parameter values for the prey were selected by random-number generation from measured probability distributions. We found that the populations of simulation results were statistically similar in the duration of the interactions to experimental measurements. A sensitivity analysis found that the model predator's performance is rapidly improved with small increases in speed. Increasing the size of the simulated arena had the greatest effect on the simulation outcome and behavioral parameters for the prey showed a relatively minor influence on the simulation results. Our findings demonstrate the power of agent-based mathematical modeling for testing hypotheses about the salient features that determine the outcome of predator-prey interactions.

3.2 Introduction

Predation is a fundamental interaction between animals with implications for the ecology and evolution of a species. Although it is broadly appreciated that the outcome of these interactions depends on how both animals sense and respond to one-another (e.g., [48, 78, 3, 81, 27, 71, 74, 17]), it is largely unclear what traits matter to the success of a predator or prey, particularly when the predator is slow. This lack of understanding may partially be attributed to the sensorimotor complexity of these coupled interactions, which challenges the ability of investigators to resolve the salient features that determine their outcome. The aim of the present study was to develop an agent-based model for the predator-prey interactions in fishes that allows for an evaluation of the roles of sensing and locomotion by both animals. The predictions of this model were tested against previous experiments [73] on the interactions between a slow predator, the red lionfish (*Pterois volitans*) as they prey upon a smaller, but faster, reef fish (*Chromis viridis*).

Models of predator-prey interactions generally consider the behavior of either the predator or prey. Weihs and Webb employed a classic game-theoretical model, the 'Homicidal Chauffeur', to consider the behavior of prey fish [92, 82]. This model predicted that prey escape in a direction that maximizes their distance from the predator, assuming that both animals move with a fixed velocity. Howland developed a model that relaxed this assumption, and instead determined the curvature of turning that allows bird prey to succeed in evading larger predators in a chase [46]. Aerial predators have also provided the focus of models for the targeting of prey, including hawks, bats, robber flies, and dragonflies [31, 14, 50, 52, 68, 37]. By comparing predicted trajectories of a predator to measurements, these studies have demonstrated that aerial predators are capable of at least two types of targeting strategies ('pure-pursuit' and 'deviated pursuit'). However, when a similar approach was applied to the study of bluefish (*Pomatomus saltatrix*), it was discovered that only a single strategy was employ by these aquatic predators [60, 35]. This strategy, known as pure pursuit,

requires merely that the predator direct its heading at the instantaneous position of the prey throughout its approach (figure 3.1,*a*). Each of these models has offered critical insight into the strategy of predator or prey, but fall short of considering the coupled nature of behavioral interactions between the two animals.

The present consideration of lionfish violates an assumption of many pursuit models that the predator moves faster than its prey. Predators that employ variations of pursuit, such as stalking, or persistent-pursuit, manage to successfully capture prey [41, 9, 44, 73]. Our experimental work has shown that the lionfish are slow predators that conform to an effective strategy of persistent pure-pursuit during behavioral experiments with faster prey fish [73], irrespective of the species of prey fish [72]. It is presently unclear how to reconcile these experimental findings with the common assumption that the predator moves more quickly than the prey [82, 92], which the present modeling will address.

Our approach represents an advance in the study of predator-prey interactions through the use of agent-based models of both predator and prey. Such models have been employed for the study of collective behavior, such as fish schools [22], and bird formations [67]. In the study of these collective behaviors, the emergent properties of the animal group are simulated by solving for the trajectories of individuals, according to the stimuli to which they are exposed and their control laws. Previous studies of the behavior of fish have shown that prey may move both in response to the predator, as well as exhibiting stochastic changes in speed and direction [82, 66]. We have incorporated these factors in numerical simulations with a Monte-Carlo approach that includes random-number generation for key kinematic parameters of swimming behavior. These random numbers draw from probability distributions of measured values from previous experiments [73]. Therefore, each individual simulation generates a unique result, but performing a series of simulations generates a population of results with characteristic features. We compared the duration of interactions by Monte-Carlo simulations against previous experiments of *P. volitans* and *C. viridis* as

a means of testing the predictions of our agent-based modeling. Our sensitivity analysis additionally evaluated the effects of behavioral parameters by predicting the changes in our populations of predictions across variation in individual parameter values.

3.3 Mathematical modeling

Here we outline the methodology for our agent-based model and describe its primary features. Both predator and prey were modeled as particles with 2D motion governed by first-order ordinary differential equations and bounded by a circular arena. Numerical solutions to these equations predict the trajectories of the two animals, given their initial positions and behavioral parameter values. In this section, we detail the relevant equations for the predator and prey (figure 3.1,*b*).

3.3.1 Modeling the predator

Lionfish move at a consistent speed, but adjust their heading continuously towards a prey fish [73]. We therefore modeled the predator speed as a fixed parameter, but devised a controller that avoids traversing the walls of the circular area while attempting to target the prey with pure pursuit. This was achieved by calculating the rate of heading change for the predator ($\dot{\theta}_{\text{pred}}$) as the sum of terms that serve to avoid collision with the arena's walls ($\dot{\theta}_{\text{wall}}$) and track the prey ($\dot{\theta}_{\text{track}}$):

$$\dot{\theta}_{\text{pred}} = \dot{\theta}_{\text{wall}} + \dot{\theta}_{\text{track}}. \tag{3.1}$$

To ensure that the predator did not exceed the circular boundary, we modeled the wall avoidance to increase exponentially as the distance to the wall (d_{wall}) approached zero, as

given by the following relationship:

$$\dot{\theta}_{\text{wall}} = K_{\text{wall}}\ \text{sgn}(\theta - \gamma)\ \exp\left(-K_{\text{turn}} d_{\text{wall}}\ |\sin\left(\theta_{\text{tan}} - \theta\right)|\right), \tag{3.2}$$

where K_{wall} and K_{turn} are constants that determine the intensity of wall avoidance, γ is the angular position of the fish with respect to the arena's center, and θ_{tan} is the angle tangent to the arena's boundary (figure 3.1*b*). The tangent angle for the predator was calculated as follows:

$$\theta_{\text{tan,pred}} = \gamma + \text{sgn}\left(\theta - \gamma\right)\ \left(\pi + |\theta_{\text{tan},0}|\right), \tag{3.3}$$

where $\theta_{\text{tan},0}$ is the offset angle from which to turn away from the wall. To model pure pursuit, the rate of change in heading due to tracking attempts to maintain a zero bearing (ϕ), as determined by the following relationship [79]:

$$\dot{\theta}_{\text{track}} = K_{\text{track}} \sin\phi, \tag{3.4}$$

where K_{track} is the tracking constant. The bearing was calculated as follows [79]:

$$\phi = \tan^{-1}\left(\frac{\sin(\alpha - \theta_{\text{pred}})}{\cos(\alpha - \theta)}\right), \tag{3.5}$$

where α is the prey's angular position relative to the predator (figure 3.1,*a*) and θ_{pred} is the predator's heading (figure 3.1). The occurrence of a strike was dependent upon both the distance between the predator and prey, and the angular position of prey with respect to the line-of-sight (α), a combination which we term the 'strike-zone'. Based on observations of lionfish striking behavior, we determined the threshold range of the bearing angle for a strike to occur within $-15° < \phi < 15°$.

3.3.2 Modeling the prey

Unlike red lionfish, the prey *C. viridis* varies both speed and heading over time [73]. We modeled the heading of the prey to avoid the walls and the predator ($\dot{\theta}_{\text{avoid}}$), in addition to routinely changing direction ($\dot{\theta}_{\text{rout}}$):

$$\dot{\theta}_{\text{prey}} = \dot{\theta}_{\text{wall}} + \dot{\theta}_{\text{avoid}} + \dot{\theta}_{\text{rout}}. \tag{3.6}$$

Wall avoidance was calculated in the same manner as for the predator (equation 3.2), but the tangent angle was calculated differently to account for spontaneous change in direction near the walls. This tangent angle was calculated by the following equation:

$$\theta_{\text{tan,prey}} = \gamma + \text{sgn}\left(\theta - \gamma\right) \left(\pi + \left|\theta_{\text{tan},0} + \hat{\theta}_{\text{tan}}\right|\right), \tag{3.7}$$

where $\hat{\theta}_{\text{tan}}$ is a randomly-generated bias angle for prey. Predator avoidance was calculated as follows:

$$\dot{\theta}_{\text{avoid}} = K_{\text{avoid}} \ \sin\left(\beta - \text{sgn}(\beta)\left|\beta_0\right|\right), \tag{3.8}$$

where β is the prey's relative heading (figure 3.1*a*), K_{avoid} is the avoidance constant, and β_0 is the avoidance heading. The relative heading is the prey's orientation relative to the line-of-sight, given by the following relationship:

$$\beta = \tan^{-1}\left(\frac{\sin\left(\alpha - \theta_{\text{prey}}\right)}{\cos\left(\alpha - \theta_{\text{prey}}\right)}\right), \tag{3.9}$$

where θ_{prey} is the prey's heading. Routine heading changes were initiated at the start of each new period of acceleration of deceleration and were determined by the following equation:

$$\dot{\theta}_{\text{rout}} = \frac{\hat{\beta}}{T}, \tag{3.10}$$

where $\hat{\beta}$ is the routine heading constant, a randomly-generated angle chosen at the beginning of an acceleration phase and T is the duration of periods of acceleration (T_{accel}) or deceleration (T_{decel}).

Consistent with experimental results [73], the prey was modeled with intermittent bouts of swimming behavior that span a series of tail-beats. Over the duration of periods of acceleration, we calculated the speed at time t during accelerations (s_{accel}) by assuming a constant acceleration (a):

$$s_{\text{accel}} = a\,(t - t_{\text{accel},0}) + s_{\text{accel},0}, \tag{3.11}$$

where $t_{\text{accel},0}$ and $s_{\text{accel},0}$ are respectively the time and speed at the initiation of a bout of acceleration. The speed values during simulations were not permitted to exceed the maximum of measured values (s_{max}). Over the periods of deceleration (for a duration of T_{decel}), the speed (s_{decel}) was modeled as a decay function, as follows:

$$s_{\text{decel}} = s_{\text{decel},0} \exp\left(\frac{t_{\text{decel},0} - t}{\tau}\right), \tag{3.12}$$

where $t_{\text{decel},0}$ and $s_{\text{decel},0}$ are respectively the time and speed at the start of deceleration period and τ is the decay constant.

3.4 Model simulations and validation

We used a numerical approach to simulate the interactions between predator and prey (figure). Here we outline the method for parameterizing the model with experimental measurements, the procedure for obtaining the numerical solutions, and the results of model validation against experimental results. This was achieved by integrating the first-order differential equations for the predator's heading (equation 3.1), and the prey's heading (equation 3.6) and speed during periods of acceleration (equations 3.11) and deceleration (equation 3.12).

We used a variable time-step solver, based on an explicit fourth-order Runge-Kutta formulation (the 'ode45' function in MATLAB, v. 2021a, Mathworks, Natick, MA, USA). The initial conditions and parameter values used in a particular simulation depended on whether we were attempting to validate the model against experiments, or were performing a sensitivity analysis, as described below.

We tested the accuracy of the model with two approaches. The first approach, called 'experiment-specific validation', evaluated the ability of the model to simulate the interactions measured in individual experiments, using particular measured kinematic parameters. The second approach, known as 'population validation', drew from distributions across all experiments to simulate the broad characteristics of interactions between *P. volitans* and *C. viridis*. For both approaches, we compared the population of simulation durations of the interaction against the measured duration of the experiments. The simulations for both approaches assumed a fixed diameter for the arena equal to the size of the previous experiments (1.2 m) [73]. A number of kinematic parameters were used for all simulations that were determined by stepwise inspection of simulation results to qualitatively match kinematic measurements (itemized in table 3.1). Simulations were performed until the prey appeared within the strike-zone of the predator, or the maximum duration transpired, which ever occurred first. The maximum duration of 300 s was used for validation, which corresponds to the period of kinematic analysis in the previous study [73]. Each simulation that ended after exceeding the maximum duration were deemed 'time-terminated', while those that ended with the predator and prey reaching the strike-zone were designated as 'strike-terminated'. Therefore, the overall strike probability of a batch of simulations could be determined by finding the proportion of strike-terminated simulation. For both approaches, we performed batches of 300 simulations to generate a population of predicted outcomes with variation generated by randomly-selected parameter values.

3.4.1 Experiment-specific validation

The simulations for the experiment-specific validation used fixed parameter values that were drawn from individual measurements specific to each experiment. This included the initial conditions of the position and heading of each fish, and the predator's strike distance. The predator was modeled with a speed equal to the mean value of the experimental measurement. The prey's changes in speed were determined by random number generation from distributions of values from within each experiment for a, T_{accel}, and T_{decel}. The only randomly-selected variable in experiment-specific validations was the change in heading ($\hat{\beta}$, equation 3.10), which was calculated at the start of each period of acceleration and deceleration. The distribution fit for this variable was based on the observations of prey behavior during experiments and represented the magnitude of a change in heading, rather than a new heading set point (figure 3.2*d*).

We compared the population of predicted outcomes against the results of 17 previous experiments [73]. For purposes of validation, we removed time-terminated simulations from this analysis because of the artificial limitations we placed on the maximum duration. The percentage of strikes measured in experiments (82%) fell within 1 S.D. of the mean proportion of strike-terminated simulations ($72\% \pm 36\%$). The mean duration of strike-terminated simulations, was not significantly different from the duration of experiments that ended in a strike ($p = 0.67$, Wilcoxon sign rank test, figure 3.2*a*). Therefore, the model simulations largely predicted the duration of our our experimental results.

3.4.2 Population validation

The population validation sought to test predictions that were general to the types of interactions characteristic of *P. volitans* and *C. viridis*. Because the population validation was not focused on simulating any particular experiment, these simulations employed a number of

variable and parameter values that were selected randomly. The random variables included the initial conditions for the position and heading of predator and prey, each with an equal probability for each position in the arena and body orientation. Strike distance was chosen from a 'log-normal' probability distribution fit (using the 'makedist' function in MATLAB) to experimental measurements (figure 3.2c).

Other random parameter values were chosen from probability distribution functions that were fit (using the 'makedist' function in MATLAB) to experimental measurements. This included parameters that determined the speed of prey: prey acceleration, acceleration duration, and deceleration duration. We extracted the mean value (μ) and standard deviation (σ) for these parameters across all bouts of acceleration and deceleration, within each experiment. Using the mean measurements from all 17 experiments, we were able to formulate a distributions of values for the mean (μ_{pop}) and standard deviation (σ_{pop}) of particular parameters. A simulation-specific probability distribution for each parameter was created at the onset of a simulation, from which particular values could be selected from within a simulation. For example, at the start of a simulation, the solver randomly selected a mean value for acceleration from the distribution of mean values, and a standard deviation value of acceleration from the standard-deviation distribution. Those mean and standard deviation values would then provide a distribution from which random values for acceleration would be chosen at the start of each period of acceleration during the simulation (figure 3.2). We additionally recorded the minimum and maximum values of each parameter across all experiments (table 3.2) and restricted the selection of random values within those bounds. The change in heading of prey ($\hat{\beta}$, equation 3.10) was randomly-generated as in the experiment-specific validations and was calculated at the start of each period of acceleration and deceleration.

The strike probability of simulations (69%, when the maximum duration was 300 s) was slightly less than the percentage of strikes within experiments (83%), but the mean duration of experiments where strikes occurred was not significantly different from that of

strike-terminated simulations ($p = 0.45$). We ran an additional population validation using batches of simulations with a maximum duration of 3600 s. This validation was used to determine a fixed maximum duration that encompassed almost all of the validated simulation duration. From this batch, we found the 85th quantile of duration, 1200 s, which was set as the maximum simulation duration for all remaining experiments. To validate the longer simulation duration, we validated a third batch of simulations and found that the strike probability of population-level simulations (80%) at this level was nearly identical to the percentage of strikes within experiments (83%). To validate simulations of longer duration, we compared the duration of strike-terminated simulations to the mean measured duration and found that the model was indistinguishable from the experimental duration ($p = 0.09$, Wilcoxon rank sum test).

3.5 Sensitivity analysis

We performed a sensitivity analysis that considered the role of behavioral traits in the outcome of predator-prey interactions. The nature of each parameter (fixed or time-variable) dictated the method in which the parameter was varied. For parameter values that did not depend on random number generation (i.e. fixed values, predator speed, tank size, constants), we set a series of predetermined parameter values, then ran a batch of simulations for each value in the series. Here, the value of the parameter of interest was set at the beginning of each batch. For a sensitivity analysis of prey swimming behaviors (determined by random number generation), the population mean (μ_{pop}) of a particular variable was changed in increments of $\pm 10\%$. The population standard-deviation distribution (σ_{pop}) was not altered. A new population probability distribution was created using the new mean value, from which simulation-level probability distribution curves were created at the start of each simulation. Simulation distributions were still truncated to the maximum and minimum measured values

to maintain biological relevance. Thus shifting μ_{pop} would shift the frequency of a particular variable value being randomly generated.

3.5.1 Predator traits

To examine the influence of the predator, we varied predator speed and K_{track}, a constant related to the control of heading during pursuit. We tested predator speeds with a range of values that spanned a near zero swimming speed, to speeds that matched the maximum measured prey speed. We found that predator speed had a strong effect on both the simulation duration and the strike probability. Small changes in speed beyond the measured mean values for experimental red lionfish resulted in the shortest simulation duration, and the strike probabilities near unity. However, increasing speed beyond this range did not return a proportional benefit for the simulated predator. For simulations where the predator speed was near zero, less than 10% of simulations within a batch were strike-terminated. Predator speed values that fell within the measured range of mean red lionfish speeds had a non-linear effect on both the duration and outcome of an interaction. As the simulated predator speed increased within the biological range of red lionfish, the simulation duration decreased rapidly, but the average duration of simulations with a positive standard-deviation of the mean red lionfish speed were not drastically different (figure 3.3*a*). Such non-linearity suggests that small increases in speed within the lower biological bounds of lionfish speed can drastically decrease the duration, but an increase in speed beyond the mean value does not have a major effect on the duration of the interaction. Increasing predator speed does increase the strike probability by 10% (figure 3.3*b*). The pursuit constant represents a metric of the predators responsiveness to the movement of a prey, but we found that a 3-fold increase in this constant had little, to no, effect on the simulation duration or the strike probability (figure 3.3*c*). It was only when the pursuit constant was half that of the validated value was there a slight increase in the simulation duration and a large increase in the

range of simulated duration. The strike probability was also less affected at lower values, but the strike probability was still within 20% of the measured mean duration (figure 3.3*d*).

3.5.2 Fixed prey traits

We examined the influence of the prey's kinematic and behavioral traits on the outcome of a simulation. Behavioral traits were described by the fixed parameters, K_{avoid}, the evasion bias angle, and the routine heading constant. The avoidance constant K_{avoid} was a metric for prey's responsiveness as they attempted to avoid the predator. Small values equated to low responsiveness to a predator, which resulted in short simulated duration, and a strike probability near 1 (figure 3.4*a,d*). As responsiveness to the predator increased, we found a positive near linear relationship of mean duration, and a similar negative relationship with the strike probability. The range in simulation duration also increased as a function of increased responsiveness. Increased evasion bias angle altered the direction changes that occurred during an interaction. Values near zero represent a strategy where prey attempts to move directly away from the predator, while values close to 180° represented a change in direction toward the predator. Evasion bias angles from 0° to 45° resulted in the longest duration, after which increased angular values corresponded to a rapid decline in duration (figure 3.4*b*). Increased evasion bias angle had a small effect on the strike probability. Bias angles below 45° resulted in a slightly lower strike probability than evasion bias angles greater than 45° (figure 3.4*e*). The routine heading constant directly affected the distribution of possible heading changes from 0° to 360°. Small values of this constant resulted in a near uniform distribution of potential angular values from 0° to 360° that could be chosen at the start of behavioral phases. Large values of the routine heading constant resulted in a distribution of possible values heavily skewed around 0°. The angle chosen during a simulation reflects a large or small magnitude in the future change of head from that of prey's prior heading. Changes in the routine heading constant had little effect on the average

duration or the strike probability (figure 3.4*c,f*). The routine heading constant increased the range of duration values within a batch, likely a reflection of increased stochasticity of the positional changes of the prey.

3.5.3 Time-variable prey traits

Traits related to the kinematics of prey were based on probability distributions of population-level kinematics, and values were randomly generated during the acceleration and deceleration phases of the prey. Acceleration duration correlated to the periods of time that a prey spend accelerating, thus a negative change in the original value of μ_{pop} caused a shortening of the acceleration phase, reducing the speed of the prey. A positive change to the acceleration duration extended the period of time a prey spent accelerating and thus increasing the speed. We found that the change in acceleration duration was similar to a mild sigmoidal distribution, where negative changes of acceleration caused a sharp reduction in the simulation duration and the range of duration. A positive change in acceleration caused small increases in the mean duration (figure 3.5*a*). The range of duration seen within batches rapidly expanded with positive changes in acceleration duration. As changes to acceleration increased in the positive direction, the strike probability decreased by 20%, with a similarly scaled increase in strike probability as the change in acceleration duration became more negative (figure 3.5*b*). Changes to μ_{pop} of acceleration at the outset of simulation directly affected the swimming speed of the prey. As the value of acceleration increased from 0 to 100% of the original value, the mean duration increased, as did the range of the duration's simulated. As acceleration was decreased by 0 to −90% of the original value, the simulation duration dropped sharply, and the duration of simulations within a batch also became shorter. We found a similar relationship between acceleration and the strike probability. For changes in acceleration from 0 to −90%, the value of acceleration decreased and the strike probability rapidly increased. However, as the change in the acceleration increased from 0 to 100%, the

probability of a strike remained similar to the probability found when acceleration was set to the original value. The deceleration duration of a prey and the decay function served to determine the instantaneous prey speed. As the μ_{pop} of deceleration was changed in the positive direction, there was a slight decrease in the average simulation duration, and a decrease in the range of duration. As the change in deceleration duration became more negative, there was an immediate increase in the simulation duration, followed by a rapid decline in duration around a percent change of -40. Thus, the average simulation duration for extreme negative changes in deceleration duration were actually lower than the average simulation duration at extreme positive changes in deceleration duration. This pattern was directly reflected in strike probability. The strike probability declined from a change in deceleration of 100% to -40%, after which there was a steep increase in the probability of a predator strike. The change in simulation duration between 0 to -40% and -40 to -100% is likely explain by a high prey speeds as the period for deceleration shortened.

3.6 Discussion

Our mathematical modeling of predator-prey interactions well replicated the simulation duration and strike outcome seen in lionfish and their prey. The model was parameterized with the results of experimental measurements (tables 3.1 and 3.2) [73] and we tested the predictions of the model for individual experiments, as well as the overall results of measured interactions (figure 3.2). Upon validating the model's predictions, we performed a sensitivity analysis to probe the effects of the model's parameters on the duration of the interactions and the probability of prey capture.

The predictions of our model were tested in ways that were both specific and general to the conditions of our experiments from a previous study [73]. Simulations for our experiment-specific validation used the initial position and heading of the fish and kinematic parameters

from the measurements within individual experiments. For most of those experiments, the measured duration of an experimental interaction was not significantly different from the duration of strike-terminated simulations (figure 3.2*a*). To evaluate whether the model could accurately predict the population of experimental results, our population validation test consisted of performing a series of simulations with random initial conditions and parameter values that were drawn from distributions (tables 3.1 and 3.2), based on all experiments. The probability of prey capture was indistinguishable from the capture success seen in behavioral experiments, and the duration of strike-terminated simulations well represented the duration of experiments (figure 3.2*b*). The use of complex agent-based controllers for both predator and prey is distinct from previous studies of pursuit and evasion, where the focus is typically on reproducing the trajectories of one animal in response to the predetermined positions of the other [60, 21, 83, 14].

Our validated model afforded an opportunity to evaluate the effects of predator behavior on predator-prey interactions. The tracking constant of our model determines how readily the predator adjusts its heading in respond to a change in the prey's position (equation 3.4). There was a subtle inverse relationship between the simulation duration and the tracking constant and only the lowest values of this parameter offered a detectable influence on strike probability (figure 3.5*c*-*d*). This suggests that the interactions are affected only when the predator is exceptionally sluggish in it ability to turn, which is consistent with previous observations of lionfish behavior. Lionfish generally do not chase prey with high-curvature turns, instead they flare large, fan-like pectoral fins continuously during their slow and persistent approach [73, 39, 76]. In contrast, speed was an important mediating factor in the outcome of the simulations. A slight reduction in predator speed below the mean measured speed in experiments showed a $\sim 2.5\times$ increase in the simulation duration, whereas the same increase in speed reduced the duration almost 4-fold, due to the nonlinear dependence of duration on speed (figure 3.3*a*). Further small increases in speed reflect only small ($< 1.5\times$) decreases in average duration. Strike probability exhibited an approximately inverse

relationship to that of simulation duration, with an almost perfect strike probability at slightly faster predator speeds (figure 3.3*b*). Beyond the physiological costs of speeding up, the trade-off may be less favorable for predators with cryptic appearances. The large frontal view imposed by the pectoral fins of lionfish may induce a greater looming stimulus to prey at higher speeds, serving to startle prey [28, 61]. Increased approach speed can elevate the distance at which prey display evasive behaviors, while a slow approach may serve to delay the response of prey [18, 16, 20]. While aspects of sensory biology are not directly modeled here, predictive behaviors are helpful for reconciling physiological constraints and observed behaviors.

We considered how the control of prey heading affects predator-prey interactions. We found that the kinematics of routine swimming offered a relatively minor influence on the outcome of interactions. In particular, changes in the routine heading constant, which determines the extent of heading changes from spontaneous turns (equation 3.10), showed a modest influence on mean values of the simulation duration (figure 3.4*c*). Perhaps not surprisingly, the kinematics of avoidance showed a stronger effect on the outcome of interactions. This was apparent through manipulations of the avoidance constant, which determines the rate at which a prey turns away from a predator (equation 3.8). Our 6-fold variation in values of this parameter exhibited an even greater range of variation in simulation duration (figure 3.4*a*). Therefore, the responsiveness related to turning away from the predator's heading did succeeding in aiding predator avoidance. Variation in the avoidance heading, the angle relative to the line-of-sight at which the prey moves (equation 3.8), affected the duration and strike probability (figure 3.4*b,e*). Prey were most successful at avoiding predators when moving directly away from the predator ($\beta_0 = 0$) to a right angle to the predator's heading ($\beta_0 = 90°$). Escaping prey may attempt to maximize the distance from a predator [92, 82], or respond with random changes in heading of evasive [47]. Maximizing distance may be most effective to a prey that is faster than the predator [82], but may be less useful in confined spaces, where random encounters may be possible. Angles directed toward the predator

were, not surprisingly, less successful. Strategic and sharp turning maneuvers are common in some flying prey [46] as a way to outmaneuver a predator, but directions directly toward the prey may be risky, particularly when the suction feeding strike of many fish may reduce the distance necessary for capture [89, 42].

Our simulations additionally considered how the control of speed in prey affects the duration of their survival in interactions with lionfish. Due to the intermittent swimming of prey fish, speed was modeled as varying over time and hence was determined by the acceleration and the duration of acceleration and deceleration, whereas the rate of deceleration was governed by a fixed decay constant. All of these parameters influenced the interactions largely in the manner that might be expected. Simulations extended over longer periods of time, with a decrease in the strike probability, as the acceleration and its duration increased (figure 3.5*a*-*d*). An increase in the duration of deceleration also generated a predictable decline in the simulation duration, but an even large reduction in deceleration duration generated a surprising reduction in simulation duration as well (figure 3.5*c*). We attribute this effect to the manner in which continuous swimming increases the encounter rate between predator and prey, within the confines of the modeled arena. Future simulations are needed to determine if this trend is an artifact of a particular arena size or shape.

3.7 Summary

In summary, our agent-based model succeeded in replicating many of the features of interactions between lionfish and their prey. The duration of interactions and the strike probability were similar between experiments and strike-terminated simulations (figure 3.2). Our sensitivity analyses revealed how the model's predictions varied substantially when the predator's speed was reduced to a level slightly below that of lionfish (figure 3.3), and that the factors that govern prey speed exhibited a more subtle, but significant, effect on the interactions

(figure 3.5). In experiments with devil lionfish, the locomotor behavior of prey did not offer a predictive determination of a prey's ability to avoid lionfish [72]. Simulated strike probabilities suggest that variably between the locomotor behaviors of prey may have an effect on the time of survival but a lesser effect on overall evasion. These results support the fundamental importance of the speed of predator and the decision of prey to make changes to heading and speed in their interactions. Our modeling furthermore demonstrates the promise of agent-based models to reveal the mechanistic role that locomotion plays in predation.

3.8 Figures and tables

Table 3.1: Fixed parameter values for simulations.

parameter	units	predator	prey
τ	s	–	2
K_{wall}	rad s^{-1}	1000	1000
K_{turn}	m^{-1}	10	10
$\theta_{\text{tan},0}$	rad	0.52	0.17
β_0	rad	–	0.01
s_{max}	m s^{-1}	–	0.40
K_{track}	rad s^{-1}	1.0	–
K_{avoid}	rad s^{-1}	–	2.0

Table 3.2: Probability distribution statistics for random parameter values.

		μ_{pop}		σ_{pop}			
parameter	units	μ	σ	μ	σ	min.	max.
a	m s^{-2}	0.0394	0.0244	0.021	0.0158	0.0052	0.0935
d_{strike}	m	-2.7732	0.4090	–	–	0.0302	0.1693
T_{accel}	s	0.9985	13.65	0.6646	0.3876	0.9985	0.7280
T_{decel}	s	1.0447	0.6918	0.7426	0.4572	0.0667	2.6409

Table 3.3: Table of symbols

variable	definition
a	prey acceleration
α	angle of the line-of-sight
β	relative heading
β_0	relative heading bias
$\hat{\beta}$	routine heading constant
γ	angular position
d	distance between predator and prey
d_{strike}	strike distance
d_{wall}	distance to wall
ϕ	bearing
ϕ_0	bearing setpoint
θ	heading
θ_{tan}	wall tangent angle
$\theta_{\text{tan},0}$	wall bias angle
$\hat{\theta}_{\text{tan}}$	wall error offset angle
$\dot{\theta}_{\text{pred}}$	rate of turning in predator
$\dot{\theta}_{\text{track}}$	rate of turning in tracking
$\dot{\theta}_{\text{prey}}$	rate of turning in prey
$\dot{\theta}_{\text{avoid}}$	rate of turning for predator avoidance
$\dot{\theta}_{\text{rout}}$	rate of routine turning in prey
$\dot{\theta}_{\text{wall}}$	rate of routine turning for wall avoidance
K_{wall}	wall avoidance constant
K_{turn}	wall turning constant
K_{avoid}	avoidance constant
K_{track}	tracking constant
μ	mean
μ_{pop}	population mean
s_{behav}	prey speed
$s_{\text{behav},0}$	initial prey speed
σ	standard deviation
σ_{pop}	population standard deviation
t	time
$t_{\text{behav},0}$	behavior start time
T_{accel}	duration of acceleration
T_{decel}	duration of deceleration
τ	decay constant

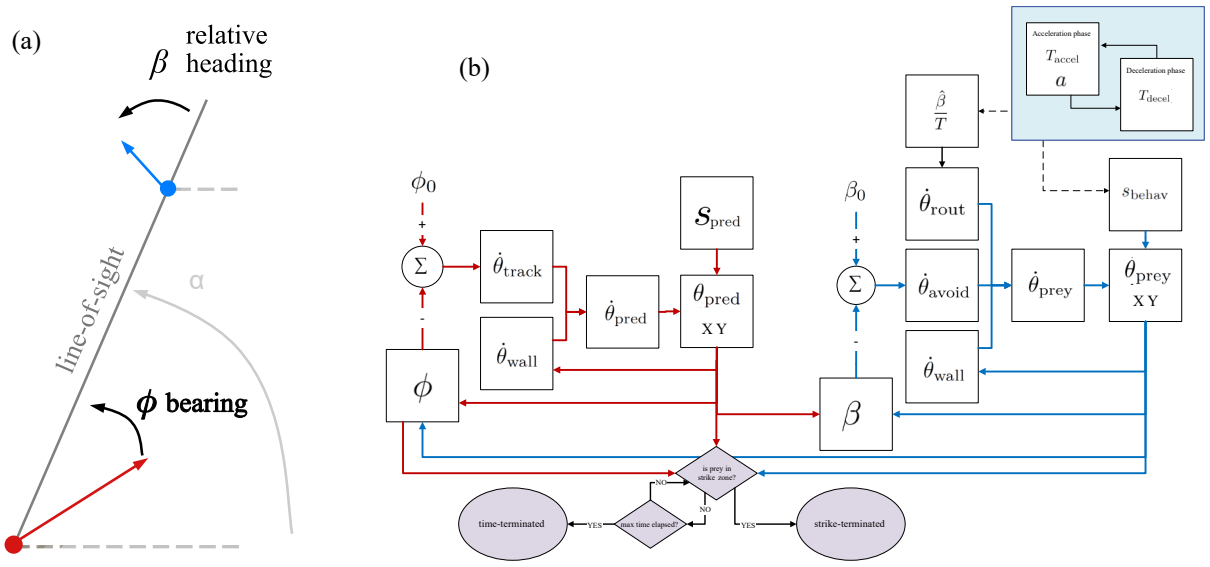

Figure 3.1: Schematic illustrations of the angles and control diagram for the predator-prey agent-based model. (a) Depiction of angles used in simulation control model, with the position of predator (red circle) and prey (blue circle) and the heading (θ, arrows), defined relative to the global frame of reference (dashed lines). The line-of-sight (grey line, at angle α) represents the prey's angular position relative to the predator. Angles related to the pursuit (the bearing, ϕ) and evasion (the relative heading, β) are found with respect to the line-of-sight. (b) Diagram of control for simulated predator-prey behaviors, with the control of simulated predator (red arrows, equations 1 to 5) and the prey (blue arrows, equations 6 to 9). Prey locomotor behavior (filled blue box) included randomly generated parameter values determined at the beginning of a behavioral phase (equations $10 - 12$). Control of simulation termination is depicted with a decision tree (filled purple), with strike-terminated simulations occurring when prey were with the strike-zone of a predator. Simulations that exceeded the maximum set duration were time-terminated. See table 3.3 for additional symbol definitions.

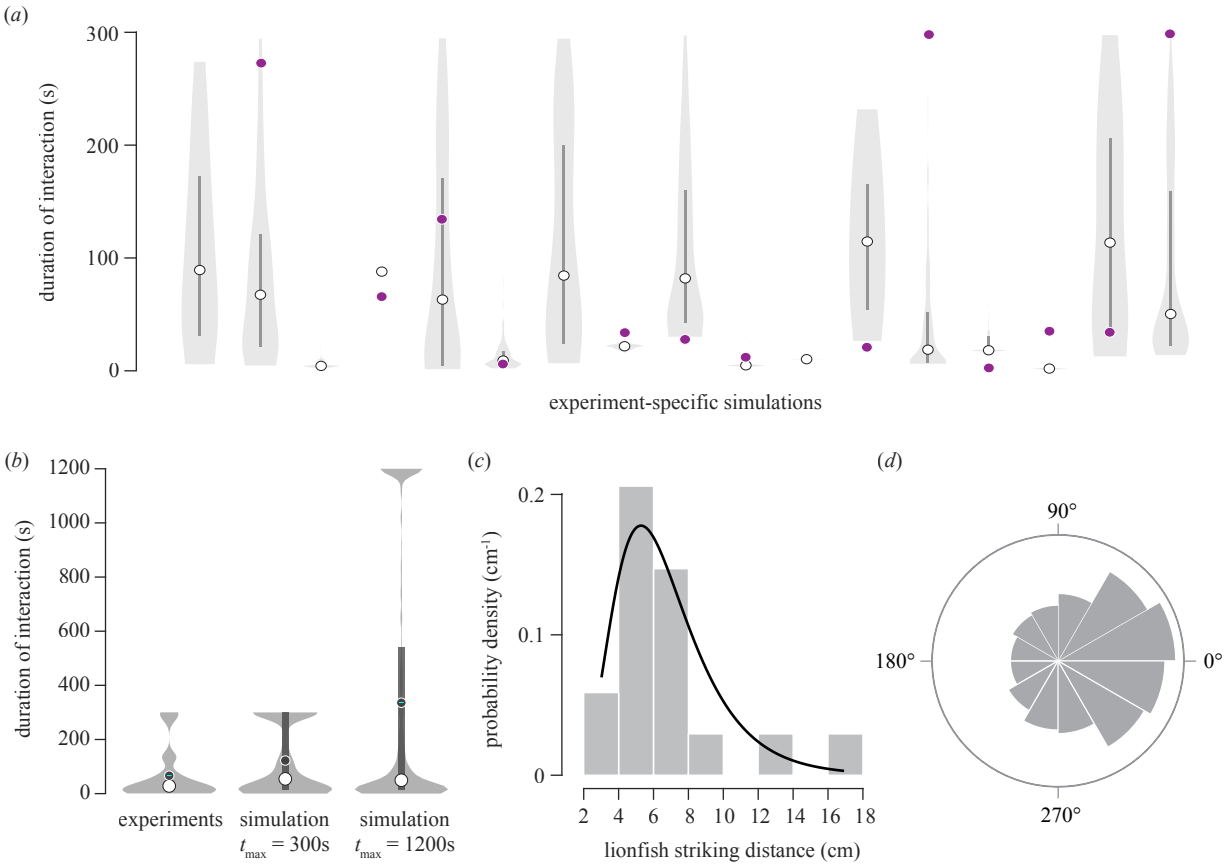

Figure 3.2: Comparison of model predictions against experimental measurements. (*a*) Experiment-specific validation, with experimental measurements (purple circles) plotted along with violin plots of simulations modeling the conditions of each experiment. Violin plots visualize distributions that include kernel density estimate of the probability density function (shaded area) with inset boxplots (vertical line) with boundaries that depict the first and third quartiles with the median value highlighted (white circle). The absence of a purple circle indicates that the individual experiment did not end in a strike, but that simulation was still able to replicate interactions that did result in a strike. (*b*) The duration of experiments and of two sets of pooled simulations are depicted with violin plots, where the maximum simulation time was capped at 300 s and 1200 s. Simulations were based on the kinematics of a species that were pooled together, where some variables pulled from distributions of kinematics. Mean values are overlaid in a black circle with white edges. (*c*) Histogram of measured red lionfish strike distance from kinematics, with a log-normal distribution curve-fit to the data (black line). (*d*) An example of the circular probability distribution used to determine the changes in prey's routine heading. The shape of the circular distribution represents the frequency that a particular angular value was chosen by circular random number generation during at the start of acceleration and deceleration phases.

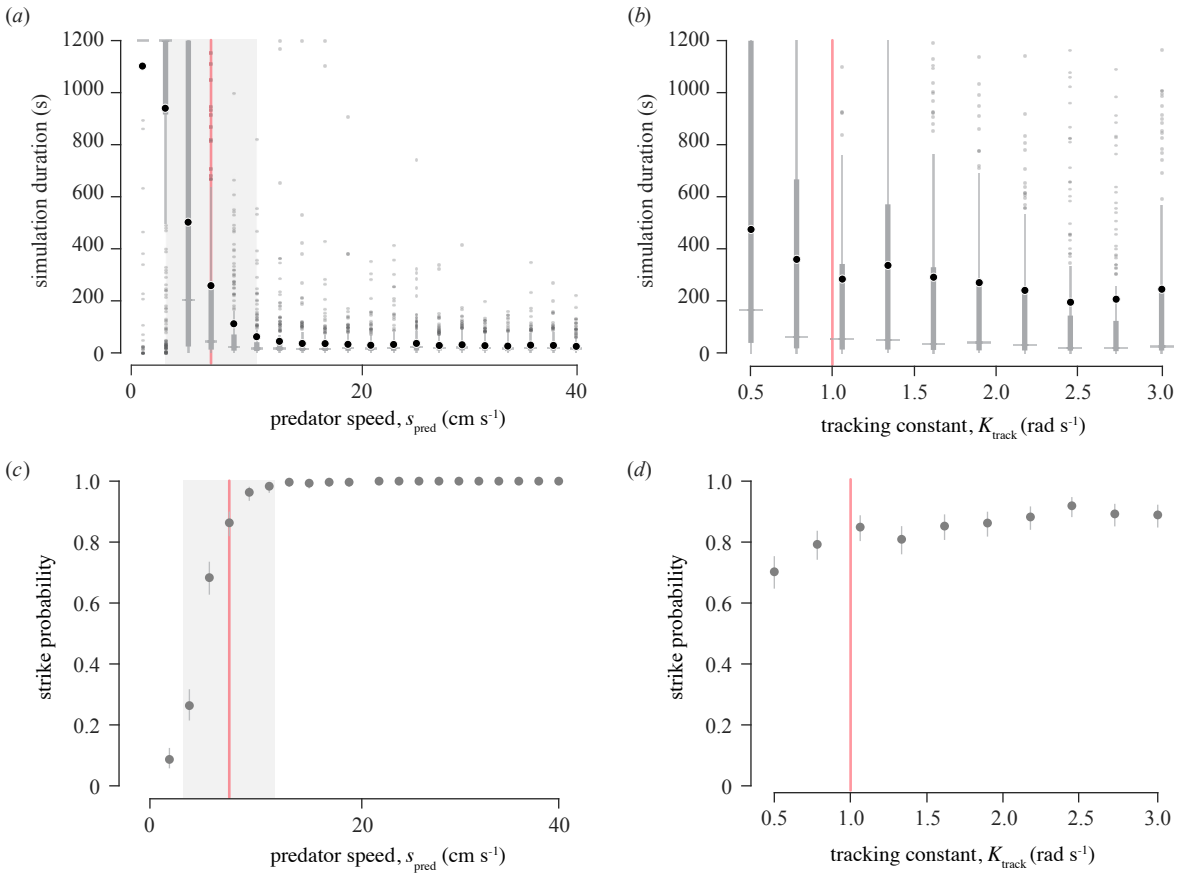

Figure 3.3: Sensitivity analysis of parameters for predator behavior. (*a*-*b*) Predator-specific parameters were varied for batches of simulations. The results for simulation duration are shown with the box plots (thick vertical gray line) depicting the first and third quartiles, whiskers (thin vertical line) indicating the range of the data, outliers (gray circles), the median value (horizonal gray line), and the mean (black circles). The mean measured value (red line) is highlighted with 1 SD (filled gray area). These results are shown for variation in (*a*) predator speed and (*b*) the tracking constant. (*c*-*d*) The probability of a predator's strike (gray circles) for each parameter value, with 95% confidence intervals (vertical grey lines), and the measured value (red line) for the (*c*) predator speed and (*b*) the tracking constant.

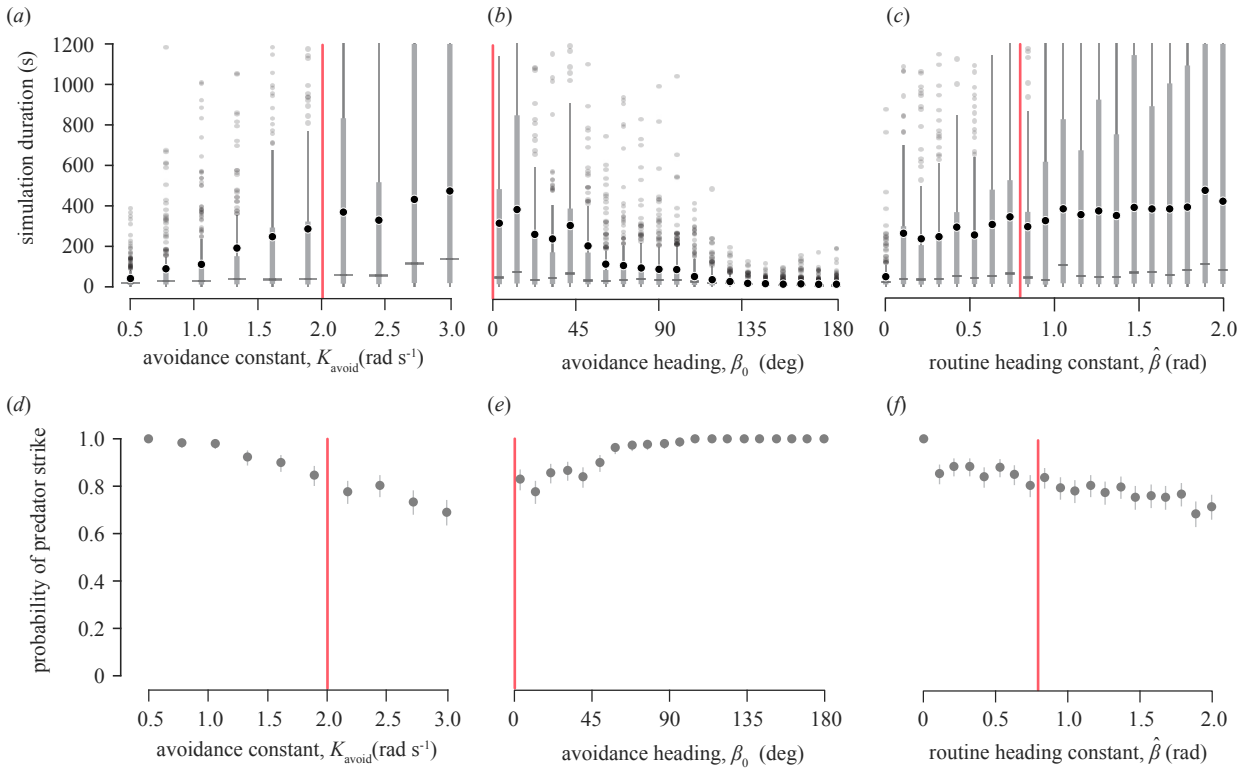

Figure 3.4: Testing the effects of prey behavior. (*a*-*c*) The simulation duration as a function of changes in parameter values of (*a*) the avoidance constant, (*b*) the avoidance bias angle, and (*c*) the routine heading constant. (*a*-*c*) The strike probability for the same simulations that varied (*a*) the avoidance constant, (*b*) the avoidance bias angle, and (*c*) the routine heading constant. All symbols are the same as in figure 3.3.

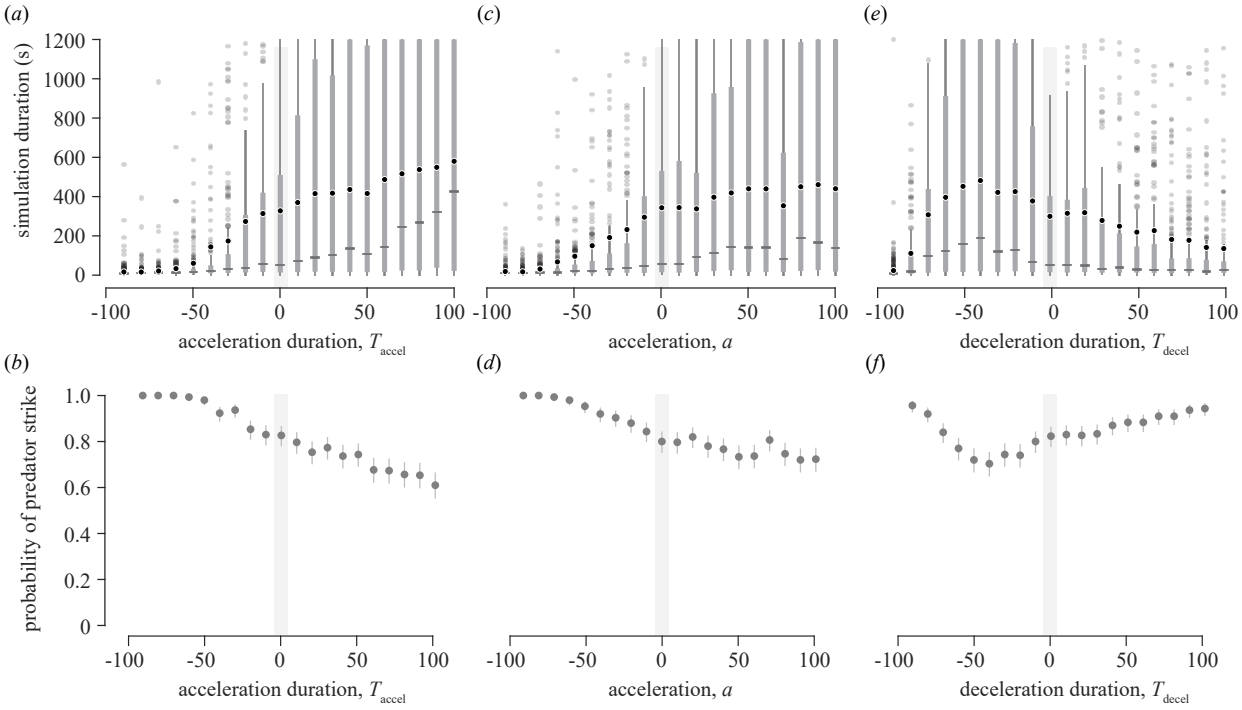

Figure 3.5: Testing the effects of prey acceleration. The simulation duration as function of the change in the mean parameter values used to create probability distributions for (a) acceleration duration, (b) acceleration, and (c) deceleration duration, from which randomly generated values for each simulation were determined. $(d\text{-}f)$ The variation in strike probability across the same simulations that varied (d) acceleration duration, (s) acceleration, and (f) deceleration duration. All symbols are the same as in figure 3.3.

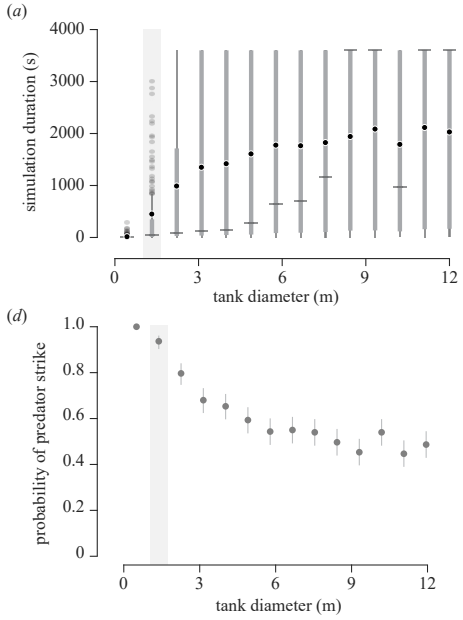

Figure 3.6: Testing the effects of tank size on simulations of extended duration. The effects of varying tank diameter are shown for (a) simulation duration and (b) strike probability. All symbols are the same as in figure 3.3.

Bibliography

[1] P. A. Abrams. The evolution of predator-prey interactions: theory and evidence. *Ann. Rev. Ecol. System.*, 31:79–105, 2000.

[2] R. M. Alexander. *Principles of Animal Locomotion*. Princeton University Press, Princeton, NJ, 2003.

[3] M. E. Alfaro. Forward attack modes of aquatic feeding garter snakes. *Func. Ecol.*, 16(2):204–215, 2002.

[4] A. Anton, K. Cure, C. Layman, R. Puntila, M. Simpson, and J. Bruno. Prey naiveté to invasive lionfish *Pterois volitans* on caribbean coral reefs. *Mar Ecol Prog Ser*, 544:257–269, 2016.

[5] E. Arndt, M. P. Marchetti, and P. J. Schembri. Ecological impact of alien marine fishes: insights from freshwater systems based on a comparative review. *Hydrobiologia*, 817(1):457–474, 2018.

[6] R. Aronson. Foraging behavior of the west atlantic trumpetfish, *Aulostomus maculatus*: use of large, herbivorous reef fishes as camouflage. *Bull. Mar. Sci.*, 33(1):166–171, 1983.

[7] P. J. Auster. Predation tactics of trumpetfish in midwater. *Neotrop. ichthyol.*, 6(2):289–292, 2008.

[8] P. Barbosa and I. Castellanos. *Ecology of predator-prey interactions*. Oxford University Press, 2005.

[9] A. Bear and O. Hasson. The predatory response of a stalking spider,*Plexippus paykulli*, to camouflage and prey type. *Anim. Behav.*, 54(4):993–998, 1997.

[10] C. E. Benkwitt. Invasive lionfish increase activity and foraging movements at greater local densities. *Mar. Ecol. Prog. Ser.*, 558:255–266, 2016.

[11] P. Berens. CircStat : a MATLAB toolbox for circular statistics. *J. Stat. Soft.*, 31(10), 2009.

[12] A. N. Black, S. R. Weimann, V. E. Imhoff, M. L. Richter, and M. Itzkowitz. A differential prey response to invasive lionfish, *Pterois volitans*: Prey naivete and risk-sensitive courtship. *J Exp Mar Biol Ecol*, 460:1–7, 2014.

[13] D. T. Blumstein. The Multipredator Hypothesis and the Evolutionary Persistence of Antipredator Behavior. *Ethology*, 112(3):209–217, 2006.

[14] C. H. Brighton, A. L. R. Thomas, and G. K. Taylor. Terminal attack trajectories of peregrine falcons are described by the proportional navigation guidance law of missiles. *Proc. Nat. Acad. Sci.*, 114(51):13495–13500, 2017.

[15] C. Chiu, P. V. Reddy, W. Xian, P. S. Krishnaprasad, and C. F. Moss. Effects of competitive prey capture on flight behavior and sonar beam pattern in paired big brown bats, Eptesicus fuscus. *J. Exp. Biol.*, 213:3348–3356, 2010.

[16] J. Cooper, W E. When and how do predator starting distances affect flight initiation distances? *Can J Zool*, 83(8):1045–1050, 2005.

[17] S. D. Cooper, D. W. Smith, and J. R. Bence. Prey selection by freshwater predators with different foraging strategies. *Can. J. Fish. Aquat. Sci.*, 42(11):1720–1732, 1985.

[18] W. E. Cooper. Dynamic Risk Assessment: Prey Rapidly Adjust Flight Initiation Distance to Changes in Predator Approach Speed. *Ethology*, 112(9):858–864, 2006.

[19] W. E. Cooper and D. T. Blumstein. *Escaping From Predators*. Cambridge Univ. Press, Cambridge, 2015.

[20] W. E. Cooper, Jr, D. Hawlena, and V. Pérez-Mellado. Interactive effect of starting distance and approach speed on escape behavior challenges theory. *Behav Ecol*, 20(3):542–546, 2009.

[21] A. J. Corcoran and W. E. Conner. How moths escape bats: predicting outcomes of predator–prey interactions. *J. Exp. Biol.*, 219:2704–2715, 2016.

[22] I. D. Couzin, J. Krause, N. R. Franks, and S. A. Levin. Effective leadership and decision-making in animal groups on the move. *Nature*, 433:513–516, 2005.

[23] K. Cure, J. McIlwain, and M. Hixon. Habitat plasticity in native Pacific red lionfish *Pterois volitans* facilitates successful invasion of the Atlantic. *Ma Ecol Prog Ser*, 506:243–253, 2014.

[24] I. M. Côté and N. S. Smith. The lionfish *Pterois sp.* invasion: has the worst-case scenario come to pass? *J. Fish. Biol.*, 92(3):660–689, 2018.

[25] D. D'Agostino, C. Jimenez, T. Reader, L. Hadjioannou, S. Heyworth, M. Aplikioti, M. Argyrou, and D. A. Feary. Behavioural traits and feeding ecology of Mediterranean lionfish and naiveté of native species to lionfish predation. *Marine Ecology Progress Series*, 638:123–135, 2020.

[26] K. A. Dahl and W. F. Patterson III. Habitat-specific density and diet of rapidly expanding invasive red lionfish, *Pterois volitans*, populations in the northern gulf of mexico. *PloS One*, 9:e105852, 2014.

[27] M. S. deVries, E. A. K. Murphy, and S. N. Patek. Strike mechanics of an ambush predator: the spearing mantis shrimp. *J. Exp. Biol.*, 215(24):4374–4384, 2012.

[28] L. M. Dill. Visual mechanism determining flight distance in zebra danios (*Brachydanio rerio* pisces). *Nat. New. Biol.*, 236(62):30–32, 1972.

[29] P. Domenici. The visually mediated escape response in fish: predicting prey responsiveness and the locomotor behaviour of predators and prey. *Mar. Freshw. Behav. Physiol.*, 35(1-2):87–110, 2002.

[30] N. El-Bakary and M. Abumandour. Visual adaptations of the eye of the gilthead sea bream (Sparus aurata). *Vet Res Commun*, 41(4):257–262, 2017.

[31] S. T. Fabian, M. E. Sumner, T. J. Wardill, S. Rossoni, and P. T. Gonzalez-Bellido. Interception by two predatory fly species is explained by a proportional navigation feedback controller. *J. R. Soc. Interface*, 15:20180466, 2018.

[32] M. Feder and G. V. Lauder. *Predator-prey Relationships: Perspectives and Approaches from the Study of Lower Vertebrates*. Chicago Univ. Press, 1986.

[33] M. C. Ferrari, F. Messier, and D. P. Chivers. Can prey exhibit threat-sensitive generalization of predator recognition? Extending the predator recognition continuum hypothesis. *Proc. R. Soc. B*, 275:1811–1816, 2008.

[34] L. A. Ferry-Graham, P. C. Wainwright, and G. V. Lauder. Quantification of flow during suction feeding in bluegill sunfish. *Zool.*, 106(2):159–168, 2003.

[35] B. A. Free, M. J. McHenry, and D. A. Paley. Probabilistic analytical modelling of predator–prey interactions in fishes. *J. Roy. Soc. Interface*, 16:20180873, 2019.

[36] T. Froukh and M. Kochzius. Species boundaries and evolutionary lineages in the blue green damselfishes Chromis viridis and Chromis atripectoralis (Pomacentridae). *J Fish Biol*, 72(2):451–457, 2008.

[37] K. Ghose, T. K. Horiuchi, P. S. Krishnaprasad, and C. F. Moss. Echolocating bats use a nearly time-optimal strategy to intercept prey. *PLoS Biol.*, 4(5):0865–0873, 2006.

[38] C. Gilbert. Visual control of cursorial prey pursuit by tiger beetles (*Cicindelidae*). *J. Comp. Physiol. A.*, 181(3):217–230, 1997.

[39] S. J. Green, J. L. Akins, and I. M. Côté. Foraging behaviour and prey consumption in the indo-pacific lionfish on bahamian coral reefs. *Mar. Ecol. Prog. Ser.*, 433:159–167, 2011.

[40] A. F. Haselsteiner, C. Gilbert, and Z. J. Wang. Tiger beetles pursue prey using a proportional control law with a delay of one half-stride. *J. Roy. Soc. Interface*, 11:20140216–20140216, 2014.

[41] M. Heurich, K. Zeis, H. Küchenhoff, J. Müller, E. Belotti, L. Bufka, and B. Woelfing. Selective predation of a stalking predator on ungulate prey. *PloS One*, 11(8):e0158449, 2016.

[42] T. E. Higham, S. W. Day, and P. C. Wainwright. Multidimensional analysis of suction feeding performance in fishes: fluid speed, acceleration, strike accuracy and the ingested volume of water. *J. Exp. Biol.*, 209:2713–2725, 2006.

[43] M. A. Hixon and J. P. Beets. Predation, prey refuges, and the structure of coral-reef fish assemblages. *Ecol. Monogr.*, 63(1):77–101, 1993.

[44] E. Hobson. *Interactions Between Piscivorous Fishes and Their Prey.* Sport Fishing Institute, Washington, DC, 1979.

[45] S. J. Holbrook and R. J. Schmitt. Effects of predation risk on foraging behavior: mechanisms altering patch choice. *J. Exp. Mar. Biol. Ecol.*, 121(2):151–163, 1988.

[46] H. C. Howland. Optimal strategies for predator avoidance: the relative importance of speed and manoeuvrability. *J. Theor. Biol*, 47:333–350, 1974.

[47] D. A. Humphries and P. M. Driver. Protean defence by prey animals. *Oecologia*, 5:285–302, 1970.

[48] R. R. Jackson. Ambush predatory behaviour of *Phaeacius malayensis* and *Phaeacius sp. indet.*, spartaeine jumping spiders (Araneae: Salticidae) from tropical Asia. *N. Z. J. Zool.*, 17(4):491–498, 1990.

[49] E. A. Kane and T. E. Higham. Modelled three-dimensional suction accuracy predicts prey capture success in three species of centrarchid fishes. *J. Roy. Soc. Interface*, 11(95):20140223, 2014.

[50] S. A. Kane, A. H. Fulton, and L. J. Rosenthal. When hawks attack: animal-borne video studies of goshawk pursuit and prey-evasion strategies. *J. Exp. Biol.*, 218:212–22, 2015.

[51] S. A. Kane, A. H. Fulton, and L. J. Rosenthal. When hawks attack: animal-borne video studies of goshawk pursuit and prey-evasion strategies. *J. Exp. Biol.*, 218:212–22, 2015.

[52] S. A. Kane and M. Zamani. Falcons pursue prey using visual motion cues: new perspectives from animal-borne cameras. *J. Exp. Biol.*, 217:225–234, 2014.

[53] I. Karplus and D. Algom. Visual cues for predator face recognition by reef fishes. *Ethology*, 55(4):343–364, 1981.

[54] T. L. Kindinger. Behavioral response of native Atlantic territorial three spot damselfish (*Stegastes planifrons*) toward invasive Pacific red lionfish (*Pterois volitans*). *Env Biol Fish*, 98(2):487–498, 2014.

[55] B. S. Lanchester and R. F. Mark. Pursuit and prediction in the tracking of moving food by a teleost fish (*Acanthaluteres spilomelanurus*). *J. Exp. Biol*, 63(3):627–645, 1975.

[56] M. Land. Chasing and pursuit in the dolichopodid fly Poecilobothrus nobilitatus. *J. Comp. Physiol. A*, 173:605–613, 1993.

[57] O. Lönnstedt and M. McCormick. Ultimate Predators: Lionfish Have Evolved to Circumvent Prey Risk Assessment Abilities. *PLoS One*, 8(10):e75781, 2013.

[58] K. Marsh-Hunkin, D. Gochfeld, and M. Slattery. Antipredator responses to invasive lionfish, pterois volitans: interspecific differences in cue utilization by two coral reef gobies. *Mar Biol*, 160(4):1029–1040, 2013.

[59] M. I. McCormick and R. Manassa. Predation risk assessment by olfactory and visual cues in a coral reef fish. *Coral Reefs*, 27:105–113, 2008.

[60] M. McHenry, J. Johansen, A. Soto, B. Free, D. Paley, and J. Liao. The pursuit strategy of predatory bluefish (*Pomatomus saltatrix*). *Proc. Roy. Soc. B*, 286:20182934, 2019.

[61] A. McKee and M. J. McHenry. The strategy of predator evasion in response to a visual looming stimulus in zebrafish (*Danio rerio*). *Integr. Org. Biol.*, 2(1):1–12, 2020.

[62] S. McTee and J. Grubich. Native densities, distribution, and diurnal activity of Red Sea lionfishes (Scorpaenidae). *Mar. Ecol. Prog. Ser.*, 508:223–232, 2014.

[63] P. Morais, M. P. P, L. Baptista, Vand R, P. Pousão-Ferreira, and M. Teodósio. Response of Gilthead Seabream (Sparus aurata L., 1758) Larvae to Nursery Odor Cues as Described by a New Set of Behavioral Indexes. *Front Mar Sci*, 4:318, 2017.

[64] M. Muller, J. W. M. Osse, and J. H. G. Verhagen. A quantitative hydrodynamical model of suction feeding in fish. *J. Theor. Biol.*, 95:49–79, 1982.

[65] P. J. Nahin. *Chases and Escapes: The Mathematics of Pursuit and Evasion.* Princeton University Press, Princeton, NJ, 2012.

[66] A. Nair, K. Changsing, W. J. Stewart, and M. J. McHenry. Fish prey change strategy with the direction of a threat. *Proc. Roy Soc. B*, 284:20170393, 2017.

[67] A. Nathan and V. C. Barbosa. V-like formations in flocks of artificial birds. *Artificial life*, 14:179–188, 2008.

[68] R. M. Olberg. Visual control of prey-capture flight in dragonflies. *Curr. Opin. Neurobiol.*, 22(2):267–271, 2012.

[69] A. N. Parker, K. A. Fritsches, C. Newport, G. Wallis, and U. E. Siebeck. Comparison of functional and anatomical estimationas of visual acuity in two species of coral reef fish. *J. Exp. Biol.*, 220(13):2387–2396, 2017.

[70] J. K. Parrish. Comparison of the hunting behavior of four piscine predators attacking schooling prey. *Ethology*, 95(3):233–246, 1993.

[71] D. Pavlov and A. Kasumyan. feeding diversity in fishes: trophic classification of fish. *J. Ichthyol.*, 42:137–159, 2002.

[72] A. Peterson, R. Holzman, and M. McHenry. Variation in locomotion among prey species has little effect on predation by lionfish (*Pterois miles*). in prep.

[73] A. Peterson and M. McHenry. The persistent-predation strategy of the red lionfish (*Pterois volitans*). *Proc B*, in review.

[74] N. N. Price and A. F. Mensinger. Predator-prey interactions of juvenile toadfish, *Opsanus tau*. *Biol.*, 197(2):246–247, 1999.

[75] P. G. Sackley and L. S. Kaufman. Effect of predation on foraging height in a planktivorous coral reef fish, *Chromis nitida*. *Copeia*, 1996(3):726–729, 1996.

[76] H. Sarhan and R. Bshary. No evidence for conspecific recruitment for cooperative hunting in lionfish *Pterois miles*. *Royal Society Open Science*, 8(9):210828.

[77] H. M. Schaefer and N. Stobbe. Disruptive coloration provides camouflage independent of background matching. *Proc. R. Soc B*, 273(1600):2427–2432, 2006.

[78] R. Shine and L.-X. Sun. Attack strategy of an ambush predator: which attributes of the prey trigger a pit-viper's strike? *Funct. Ecol.*, 17(3):340–348, 2003.

[79] N. A. Shneydor. *Missile Guidance and Pursuit : Kinematics, Dynamics and Control*. Woodhead Publishing Ltd, Haifa, Israel, 1998.

[80] A. Sih, D. I. Bolnick, B. Luttbeg, J. L. Orrock, S. D. Peacor, L. M. Pintor, E. Preisser, J. S. Rehage, and J. R. Vonesh. Predator-prey naïveté, antipredator behavior, and the ecology of predator invasions. *Oikos*, 119(4):610–621, 2010.

[81] D. J. Slip and R. Shine. Feeding habits of the diamond python, *Morelia s. spilota*: ambush predation by a boid snake. *J. Herpetol*, 22(3):323–330, 1988.

[82] A. Soto, W. J. Stewart, and M. J. McHenry. When optimal strategy matters to prey fish. *Integr. Comp. Biol.*, 55(1):110–120, 2015.

[83] A. P. Soto and M. J. McHenry. Pursuit predation with intermittent locomotion in zebrafish. *J. Exp. Biol.*, 223:jeb.230623, 2020.

[84] W. J. Stewart, G. S. Cardenas, and M. J. McHenry. Zebrafish larvae evade predators by sensing water flow. *J. Exp. Biol.*, 216:388–398, 2013.

[85] R. Svanbäck, P. Wainwright, and L. Ferry-Graham. Linking cranial kinematics, buccal pressure, and suction feeding performance in Largemouth Bass. *Physiol. Biochem. Zool.*, 75(6):532–543, 2002.

[86] H. P. A. Sweatman. A field study of the predatory behavior and feeding rate of a piscivorous coral reef fish, the lizardfish *Synodus englemani*. *Copeia*, pages 187–194, 1984.

[87] I. Temizer, J. C. Donovan, H. Baier, and J. L. Semmelhack. A visual pathway for looming-evoked escape in larval Zebrafish. *Curr. Biol.*, 25(14):1823–1834, 2015.

[88] J. Van Leeuwen and M. Muller. Optimum sucking techniques for predatory fish. *Trans. Zool. Soc. London*, 37(2):137–169, 1984.

[89] P. Wainwright, A. M. Carroll, D. C. Collar, S. W. Day, T. E. Higham, and R. A. Holzman. Suction feeding mechanics, performance, and diversity in fishes. *Integr. Comp. Biol.*, 47:96–106, 2007.

[90] P. C. Wainwright, L. Ferry-Graham, T. B. Waltzek, A. M. Carroll, C. D. Hulsey, and J. R. Grubich. Evaluating the use of ram and suction during prey capture by cichlid fishes. *J. Exp. Biol.*, 204(17):3039–3051, 2001.

[91] P. Webb. Locomotion and predator-prey relationships. In M. Feder and G. V. Lauder, editors, *Predator-prey relationships*. Chicago University Press, Chicago, 1986.

[92] D. Weihs and P. W. Webb. Optimal avoidance and evasion tactics in predator-prey interactions. *J. Theor. Biol.*, 106:189–206, 1984.

[93] A. Whitfield, J. Panfili, and J. Durand. A global review of the cosmopolitan flathead mullet *Mugil cephalus* Linnaeus 1758 (Teleostei: Mugilidae), with emphasis on the biology, genetics, ecology and fisheries aspects of this apparent species complex. *Rev Fish Biol Fisheries*, 22(3):641–681, 2012.

[94] J. H. Zar. *Biostatistical Analysis*. Prentice Hall, Upper Saddle River, N.J., 1999.

[95] S. W. Zhang, W. Xiang, L. Zili, and M. V. Srinivasan. Visual tracking of moving targets by freely flying honeybees. *Vis. Neurosci.*, 4:379–386, 1990.

Appendix A

Chapter 1 Supplemental Material

A.1 Animal care

Red lionfish (*Pterois volitans*, $n = 5$) and *C. viridis* (*Chromis viridis*, $n = 23$) were sourced from the ornamental fish trade and housed in 75 L tanks (25°C, 33.188 ppt). Lionfish were housed in individual tanks and the *C. viridis* were housed in small groups. The two species were held in separate recirculating aquarium systems to avoid acclimation to any potential olfactory or visual cues. When not running experiments, lionfish were fed an alternating diet of squid, shrimp, or silversides every-other day and the *C. viridis* were fed an enriched diet daily. During a period when experiments were conducted, the lionfish were allowed to pursue a maximum of two prey in a 24 hr period. Lionfish have highly expansive stomachs and were therefore unlikely to be fully satiated within this period.

A.2 Behavioral experiments

Experiments ($n = 23$) were conducted over two periods of activity, with each period employing slightly different experimental conditions. The experimental setup was upgraded between periods due to the acquisition of lionfish that were too large for the original arena. Lionfish were more that 5× greater in length ($n = 5$, mean total length, TL = 17.6 cm ±5.0 cm, this and all further measurements are reported as Mean ±1 SD) than the *C. viridis* ($n = 23$, TL = 3.4 cm ±0.7 cm). *C. viridis* size did not vary significantly between the two experimental periods ($p = 0.75$, Wilcoxon rank sum test). However, lionfish in the early experiments (TL = 14.8 cm ±2.1 cm, $n = 2$) were substantially smaller that in the later experiments (TL = 22.8 cm ±0.1 cm, $n = 3$). For both periods of experiments, a single lionfish and single *C. viridis* were placed in a cylindrical arena and permitted to interact, until a prey was consumed, or 1 hr had elapsed, whichever occurred first. The motion of predator and prey was filmed with a camera placed above the arena. In cases when a *C. viridis* survived the experiment, prey were not reused in another experiment ($n = 9$).

In the early experiments ($n = 6$), the arena ($\varnothing \sim 0.6\,\text{m}$, 0.2 m depth) was recorded with a VGA camera (640×40, Pike $F-032B$ with 12.5 mm lens, Allied Vision Technologies, Exton, PA, USA), at either 15 fps or 30 fps. Videos were streamed to a computer and recorded with software (StreamPix 5, NorPix, Inc., Montreal, Quebec, Canada). A single experiment was filmed in HD resolution (1920×1080) at 60 fps with a DSLR camera (Sony Alpha, A7SIII, Sony Electronics Inc., San Diego, CA, USA). To begin each experiment, lionfish and *C. viridis* were separated by an opaque divider and allowed to acclimate in the arena for 1 hr. After this period, the lionfish was corralled within a bucket, the divider was removed, and the predator was released. Lionfish were rarely startled and careful capture and re-release did not deter them from pursuing prey.

In later experiments ($n = 17$), the upgraded arena ($\varnothing \sim 1.2\,\mathrm{m}$, $0.3\,\mathrm{m}$ depth) was filmed in 4k resolution (3840×2160) at 30 fps with a DSLR camera (Sony Alpha, A7SIII or A7RIII, Sony Electronics Inc., San Diego, CA, USA) using an external recorder (Atomos Ninja Flame, ATOMOS Global Pty Ltd, Los Angeles, CA, USA). A mesh lid was positioned just below the water's surface to prevent ripples that were otherwise generated by the dorsal fin of the large lionfish. Handling this lid required that the lionfish be introduced to the arena prior to the prey, but we first allowed the *C. viridis* to acclimate in the illuminated arena alone for 1 hr. At the end of the acclimation period, all lights were turned off (with the exception of a dim red light) and the prey was removed in a large bucket. Preliminary experiments showed that lionfish failed to locate prey under these lighting conditions. This allowed us to place the lionfish into the arena, then introduce the prey, and control the start of the experiment by activating white lights that surrounded the arena. We tested for differences between the two experimental setups by comparing the subsample duration of the interactions between lionfish and *C. viridis*. We found that this duration was not significantly different ($p = 0.151$, Wilcoxon rank sum test), which suggests that any difference between the two setups was negligible.

A.3 Kinematic analysis

We performed a kinematic analysis of the events leading up to prey capture to identify the pursuit strategy of the lionfish. This analysis focused on the 5 min before capture, if the predator was successful, or the time when a failed predator reached the closest distance to the prey in experiments where there was no capture. We extracted the trajectories of each fish's center-of-area using a semi-automated tracking program written in MATLAB (v. 2019b, MathWorks, Natick, MA, USA).

The automated portion of our tracking software required manual user input to set initial parameters. An interactive graphical interface allowed the user to manually mark initial x- and y-coordinates for the body position of each fish from the first frame of a video. The diameter of a region of interest (ROI) was then chosen to encompass each fish, which served as the primary search region for the 'blob' tracking analysis. For each recording, a single mean image was compiled from the video frames (up to 100 frames) and used for background subtraction. A user-chosen contrast difference between the fish blobs and the mean image was used to create a binary image of each video frame. The contrast threshold value was determined based on a sample of nine frames pulled throughout the video duration.

The software stepped through each video frame to track the positional changes of predator and prey using a combination of binary image thresholding and 'blob' area-tracking. After conversion of a video frame to a binary image, the centroid coordinates of all blobs within the ROI diameter were calculated and the blob that best-matched the area of the prior video frame was selected for initial tracking and the pixel area of each fish was measured from nine representative frames from the video for user approval. All blobs within the ROI were surveyed and those within a designated area range were recorded. If more than one blob was found, the blob with the closest centroid to the blob in the prior frame was chosen. If no blob was found within the ROI, the tracking code expanded the survey to the full frame, and the closest blob matching the area conditions was chosen. The heading (θ_{pred}) of the lionfish body in each frame was found using image registration (the 'imregister' function in MATLAB). This approach used the predator's image from the first frame to find the body rotation in subsequent frames. Upon completion, for each video frame the blob of each fish was overlaid on the original video frame and a full movie was compiled for user approval. Fish position was manually selected with an interactive subroutine in MATLAB for a small number of frames that could not be automatically tracked.

A.4 Analysis of strategy

A cubic spline fit (the 'spline' function in MATLAB) of the coordinates of each fish were evaluated with respect to time by finding the first-derivative (the 'fnder' function MATLAB) of position, to determine velocity. The total time each fish spent below a near-zero swimming velocity was determined for each experiment. The threshold for near-zero velocity was chosen based on mean prey size and prey swimming speed, and encompassed measured swimming velocities from both predator and prey. The proportion of time each fish spent stopped was found by dividing the total time stopped by the subsample duration.

The distance between predator and prey coordinates was continuously measured. Each experiment was analyzed for the presence of an 'alternative minimum distance' (d_{alt}). This distance represented the singular closest proximity between predator and prey where the predator did not attempt a strike. d_{alt} was found using an inverted peak-finding analysis (the 'findpeaks' function in MATLAB) and was used to determine whether the distance at which lionfish choose to strike was significantly different than other minima in predator-prey distance. Experiments where the distance between lionfish and *C. viridis* declined in a linear fashion did not have a d_{alt}. Additionally, coordinate points were manually selected for the predator's rostrum and the prey's center of area from the video frame at the time of d_{alt} and from the strike frame (or final frame, if a strike was not attempted).

We calculated kinematic variables related to pursuit strategy from the trajectories of each fish. The line-of-sight between the animals was defined by the body position of the prey relative to the body position of the predator. The prey's orientation (θ_{prey}) was determined by the direction of the prey's velocity vector. The prey's orientation with respect to the predator's position was deemed the prey's relative heading (β) and found as follows:

$$\beta = \tan^{-1}\left(\frac{\sin\left(\alpha - \theta_{\text{prey}}\right)}{\cos\left(\alpha - \theta_{\text{prey}}\right)}\right), \tag{A.1}$$

where θ_{prey} is the prey's orientation and α is the angle of the line-of-sight relative to an inertial frame of reference.

The orientation of a predator relative to the prey's position is referred to as the bearing angle (ϕ), and is the focus for determining a predator's strategy. The bearing angle was determined as follows:

$$\phi = \text{sgn}(\dot{\theta}_{\text{pred}}) \tan^{-1} \left(\frac{\sin(\alpha - \theta_{\text{pred}})}{\cos(\alpha - \theta_{\text{pred}})} \right), \tag{A.2}$$

where α is the line-of-sight angle, θ_{pred} is the predator's heading, and $\dot{\theta}_{\text{pred}}$ is the rate of change of θ_{pred}. 'sgn' refers to the sign of $\dot{\theta}_{\text{pred}}$, such that the heading is directed to the left ($\text{sgn}(\dot{\theta}_{\text{pred}}(t)) = 1$) or right ($\text{sgn}(\dot{\theta}_{\text{pred}}(t)) = -1$) of the line-of-sight.

A.5 Statistical analysis

Kinematic data was tested for normality using One-sample Kolmogorov-Smirnov tests prior to statistical analyses. Data did not follow a normal distributions and were evaluated using non-parametric statistical methods. Mann-Whitney U-test (also known as Wilcoxon rank sum test) was used to evaluate relationships between independent variables, such as average predator and prey speed or capture and miss striking distance. A Wilcoxon Sign Rank Test was used for paired kinematic data, such as significance between the alternative minimum distance and striking distance within experiments. Angular data was evaluated with circular statistics, specifically employing the 'CircStat' toolbox available for use in MATLAB [11]. Predicted bearing angles were evaluated with measured bearing angles using a Model II linear regression (reduced major axis regression). This method evaluates variables that are subject to measurement error, without assuming dependence, such as a measurement and a prediction.